Title
Electrocatalysts for Oxygen Electrodes

Author
Yeager, E.

Publication Date
1993-02-01

LBL-33814
UC-331

Lawrence Berkeley Laboratory

UNIVERSITY OF CALIFORNIA

ENERGY & ENVIRONMENT DIVISION

Electrocatalysts for Oxygen Electrodes

E. Yeager

February 1993

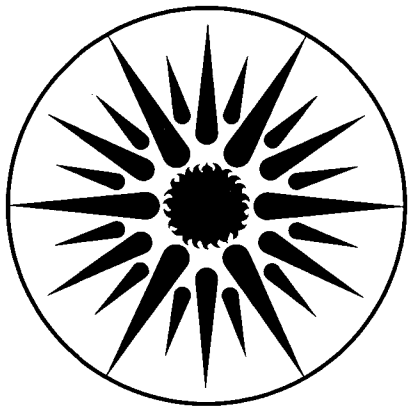

ENERGY & ENVIRONMENT DIVISION

Prepared for the U.S. Department of Energy under Contract Number DE-AC03-76SF00098

DISCLAIMER

LBL-33814

ELECTROCATALYSTS FOR OXYGEN ELECTRODES

Final Report

February 1993

by

Ernest Yeager

Case Center for Electrochemical Sciences
and the Department of Chemistry
Case Western Reserve University
Cleveland, Ohio 44106-7078

for

Exploratory Technology Research Program
Energy & Environment Division
Lawrence Berkeley Laboratory
Berkeley, California 94720

This work was supported by the Assistant Secretary for Conservation and Renewable Energy, Office of Transportation Technologies, Electric and Hybrid Propulsion Division of the U.S. Department of Energy under Contract No. DE-AC03-76SF00098, Subcontract No. 4566910 with the Lawrence Berkeley Laboratory.

PREFACE

This final report includes the important technological and scientific accomplishments of this project for the period 1 April 1984 to 30 April 1992 and a comprehensive summary of the research carried out during the past year (1 May 1991 - 30 April 1992). The list of research publications and Ph.D. dissertations obtained under this project are also given. Various active catalyst systems for the O_2 reduction and generation in concentrated alkaline and acid electrolytes as well as for the decomposition of peroxide in alkaline solutions are mentioned in appendices A and B.

The following personnel were involved in the research on a full or part-time basis.

W. Aldred	Research Assistant
R. Chen	Graduate Student
H. Huang	Graduate Student
Z. Zhang	Graduate Student
S. Gupta*	Senior Research Associate
D. Tryk	Senior Research Associate
E. Yeager	Project Director

*Report prepared by S. Gupta

TABLE OF CONTENTS

TABLE OF CONTENTS
(Continued)

I. IMPORTANT TECHNOLOGICAL AND SCIENTIFIC ACCOMPLISHMENTS OF THIS PROJECT FOR THE PERIOD 1 APRIL 1984 TO 30 APRIL 1992

This project on electrocatalysts for oxygen electrodes at CWRU was initiated in April 1984 with the objective to understand the factors controlling the activity of O_2 reduction and generation electrocatalysts and the use of this information to achieve higher activity combined with long-term stability. Two broad classes of catalysts were developed: (1) transition metal macrocycles in monomeric and polymeric forms, and (2) transition metal oxides including perovskites and pyrochlores. A new level of understanding of the electrochemical properties of these catalysts and the mechanistic aspects of O_2 reduction and generation on these catalysts has been achieved. Extensive studies were also carried out on carbons and graphite as O_2 electrocatalysts and substrates for electrocatalysts in alkaline solution. Some of the important specific accomplishments of this research are:

- Iron phthalocyanine (FePc) and its modified forms such as iron tetrasulfophthalocyanine (FeTsPc) and iron tetrapyridinoporphyrazine (FeTPyPz) catalyze the 4-electron reduction of O_2 to OH^- in alkaline solution when adsorbed on pyrolytic graphite at mono- or submonolayer coverages.
- Lead-ruthenate pyrochlores in the high-area form are very active bifunctional catalysts for O_2 electrodes in reduction and generation modes in concentrated alkaline solutions. They catalyze the 4-electron reduction of O_2 to OH^-.
- Transition metals (e.g., Co, Fe) adsorbed on heat-treated polyacrylonitrile (PAN)-based catalysts, particularly Co/PAN/XC-72, show promising performance for O_2 reduction in alkaline and acid electrolytes. These catalyst systems function through a peroxide mechanism similar to that involved with the heat-treated cobalt porphyrins and have comparable apparent activity.

- Heat-treated transition metal macrocycles such as CoTMPP dispersed on high-area carbon have high activity for O_2 reduction in alkaline and acid electrolytes, with good stability in concentrated alkaline solutions.
- The combined use of FTIR, laser Raman, TEM, Mossbauer, extended X-ray absorption fine structure (EXAFS), magnetic susceptibility, pyrolysis-gas chromatograph-mass spectroscopy and linear sweep voltammetry of the adsorbed catalyst has provided new insight into the effects of heat treatment on catalysts stability.
- Based on various electrochemical and non-electrochemical studies of the heat-treated macrocycles and related complexes, CWRU proposed a model to explain the catalytic activity of the heat-treated transition metal macrocycles. The model proposed is that of a modified carbon surface on which transition metal ions are adsorbed, principally through interaction with residual nitrogen derived from the heat-treated macrocycles.
- *Ex situ* and *in situ* Mossbauer spectroscopy was used successfully at CWRU to determine the state of the transition metal in macrocycles both in bulk and adsorbed on high-area carbon with or without subsequent heat treatment.
- FePc and its μ-oxo derivatives were characterized at Case using FTIR, Mossbauer, STM, cyclic voltammetry, RRDE and gas-fed electrode measurements. It was found that the activity associated with the μ-oxo (1) species (crystallized from DMF solution) is comparable to that obtained with Powercat 2000 (a commercially available high-area Pt-based high-performance catalyst) in alkaline solution.
- Materials produced by the heat treatment of pyrrole black mixed with transition metal salts are promising catalysts for O_2 electroreduction in both alkaline and

acid electrolytes. Their activity is comparable to that of the corresponding transition metal macrocycles which are heat treated on carbon.

- The stability of gas-fed O_2 electrodes in the reduction as well as generation modes has been enhanced by using ion conducting polymers in concentrated acid and alkaline electrolytes. This was achieved by incorporating the ionomer in the active layer of the gas-fed electrodes and also by covering the solution side of the active layer with an ionomeric membrane.
- O_2 reduction to peroxide was examined in aqueous alkaline solution on highly oriented pyrolytic graphite (HOPG) with adsorbed 9, 10-phenanthrenequinone and on ordinary pyrolytic graphite (OPG) with chemically attached 2-amino anthraquinone. The kinetics of the initial one electron transfer to the quinone on the surface with the adsorbed quinone are fast, while the reaction of the reduced quinone radical with the solution-phase O_2 is the rate determining step. For the overall $2e^-$ reduction to peroxide on the chemically attached quinone surface, the initial electron transfer is the rate determining step because the quinone is farther from the surface and in an unfavorable configuration for electron tunneling.
- O_2 reduction to superoxide was examined in acetonitrile on the basal planes of ordinary and highly oriented pyrolytic graphite. The reaction has a lower apparent cathodic transfer coefficient on HOPG than OPG, probably because part of the potential drop across the electrode-electrolyte interface occurs in the space charge region in the HOPG. O_2 reduction to superoxide in DMSO was also studied on OPG, Au and Pt electrodes with and without CoTsPc in solution. The results indicate that CoTsPc does not catalyze the O_2 reduction to O_2^- in aprotic solvents and the reaction appears to occur by an outer-sphere electron-transfer mechanism.

- Another class of compounds which has activity similar to the corresponding monomeric Pc's, and which is expected to have better stability in concentrated acid and alkaline electrolytes, is the polymeric phthalocyanines. Cobalt and iron phthalocyanine sheet-type polymers were synthesized and purified as described in the literature. They were separated from the low-molecular-weight fractions from their solutions in DMF. The high-molecular-weight fraction was characterized by FTIR, laser Raman, uv-visible and XPS measurements. The sheet-type configuration of the CoPc oligomer is evident by high-resolution transmission electron microscopic (TEM) and atomic force microscopic (AFM) measurements.
- The orientation of the macrocycle complex on the surface has a strong effect on the activity as well as the pathway for O_2 reduction. *In situ* SERS, FTIRRAS and STM measurements of monomeric TsPc's adsorbed on a substrate at mono- or submonolayer coverages provide evidence that the plane of the adsorbed TsPc complex is oriented at an angle to the surface. Polymeric sheet-type phthalocyanines, however, in the form of crystallites on a graphite surface show the sheet-shaped structure of the molecules that are stacked parallel to each other and parallel to the substrate by using AFM.
- The voltammetric peaks for the solution-phase species of CoTsPc and FeTsPc were not obtained so far in aqueous electrolytes. However, the voltammetric peaks were obtained for these species in organic solvents. A possible explanation for this was based on the excess negative charge associated with the ligand in aqueous electrolyte as a result of the ionized SO_3^- groups attached to the four aromatic rings. The adsorption of such highly charged species on the electrode surface results in the repulsion of the corresponding solution-phase

species. This explanation is supported by the effect of adsorbed TsPc's on the redox behavior of negatively charged (ferri and ferrocyanide), uncharged (o-tolidine) and positively charged $Fe(ClO_4)_3$ in aqueous acid and alkaline solutions.

- Adsorption of FeTsPc and CoTsPc on OPG was investigated as a function of pH and ionic strength of the adsorption solution as well as potential. Adsorption of CoTsPc occurs readily from its freshly prepared aqueous solution and is generally independent of pH. For FeTsPc, however, adsorption does strongly depend on pH. High surface coverage is achieved only from acid solutions rather than from pure water or alkaline solutions. This is explained in terms of the form(s) of the complexes existing in the solution phase in air.
- To obtain further insight into the redox properties and O_2 reduction electrocatalysis on macrocycles, the effect of CN^-, which is capable of coordinating with the transition metal in the axial position, was examined. The results indicate that a strong axial interaction of O_2 with the transition metal in the macrocycle is an important factor for O_2 electrocatalysis. The blocking effect of the voltammetric peaks confirms the assignment of the peaks in cyclic voltammetry curves and the importance of particular redox couple to the O_2 electrocatalysis.
- The polyvinyl pyridine (PVP)-modified OPG electrode with adsorbed CoTsPc exhibits higher activity for O_2 reduction than the OPG electrode with only adsorbed CoTsPc in 0.05 M H_2SO_4 solution. This is due to the formation of an adduct between PVP and CoTsPc which is more active and more stable than CoTsPc. FTIR and uv-visible spectroscopic studies provide evidence for the formation of an adduct between CoTsPc and PVP.

- The perovskites have not generally been found to be active catalysts for O_2 reduction in gas diffusion O_2 cathodes either with or without high-area carbon. Some of the higher-area compounds have considerable activity for peroxide decomposition and O_2 generation. When used in conjunction with heat-treated macrocycles (even macrocycles without a transition metal center), some of the perovskites show excellent performance for O_2 reduction.
- The effects of alcohols such as methanol, isobutanol and n-amyl alcohol were examined to obtain a better understanding about the redox properties and O_2 reduction electrocatalysis on transition metal macrocycles. These alcohols may change the structure of the interface and orientation of the adsorbed macrocycles on the surface. The effect of methanol and its reaction intermediates on O_2 reduction are also of interest for the identification of methanol-tolerant electrocatalysts for O_2 reduction in methanol-air fuel cells. For O_2 reduction on CoTsPc in an alkaline electrolyte, which was pre-adsorbed on an OPG disk electrode from a 0.1 M NaOH solution containing CoTsPc (~1 x 10^{-4} M) in these alcohols, the half-wave potential ($E_{1/2}$) is more positive (~60 mV). This may be due to the increased adsorption of the macrocycle on the surface as a result of changes in the dielectric property of the solvent. The presence of ~1 M methanol in 2.5 M H_2SO_4 at 60°C showed no effect on the O_2 reduction performance in gas-fed electrodes based on pyrolyzed macrocycles (CoTMPP and CoTAA adsorbed on high-area carbon). This is quite encouraging for air electrodes in acid electrolyte methanol-air fuel cell.
- A host of techniques, both electrochemical and non-electrochemical along with spectroscopic techniques, were used to characterize the most promising electrocatalysts for O_2 electrodes. These techniques include:

1. linear sweep voltammetry (LSV) and differential pulse voltammetry (DPV)
2. rotating disk electrode (RDE)and rotating ring-disk electrode (RRDE)
3. Fourier transform infrared (FTIR) spectroscopy
4. uv-visible spectroscopy
5. surface enhanced Raman scattering (SERS) and resonance Raman (RR)
6. scanning tunneling microscopy (STM) and atomic force microscopy (AFM)
7. high resolution transmission electron microscopy (HRTEM)
8. scanning electron microscopy (SEM)
9. X-ray absorption fine structure (XAFS)
10. Mossbauer effect spectroscopy (MES)
11. X-ray diffraction (XRD)
12. X-ray photoelectron spectroscopy (XPS) and ultraviolet photoelectron spectroscopy UPS
13. secondary ion mass spectroscopy (SIMS)
14. pyrolysis-gas chromatograph-mass spectroscopy (PGCMS)
15. thermogravimetric analysis (TGA)
16. magnetic susceptibility
17. elemental analysis
18. BET surface area
19. extraction techniques
20. adsorption techniques

- Pt catalysts supported on lead-ruthenate pyrochlore and with a Nafion 117 (DuPont) membrane pressed against the electrolyte side of the gas-fed electrode showed promise for bifunctional O_2 electrodes in acid electrolyte (2.5 M H_2SO_4 at 60°C).
- The fabrication of porous gas-fed electrodes was modified to optimize their stability and performance at high current densities in 85% H_3PO_4 at 100°C using carbon supported Pt catalysts for O_2 reduction and generation.
- The RRDE experiments show that the reduction of O_2 proceeds by a 4-electron pathway on Ru in alkaline electrolytes. The kinetics and mechanism depend on the oxidation state of the Ru surface. The reaction mechanisms for the formation of the anodic film and O_2 reduction on Ru are proposed.

- Lithiated NiO powder was examined as a support for Pt-catalyzed gas-fed electrodes. The performance for O_2 reduction is inferior to that obtained using carbon supports in 5 M KOH at 25°C. This oxide has negligible activity for O_2 reduction at room temperature but has significant activity for O_2 reduction at temperatures higher than 150°C. Such a p-type oxide is not expected to be active for O_2 reduction.
- CoTsPc adsorbed on the perovskite $LaCoO_3$ and $La_{0.5}Sr_{0.5}MnO_3$ powders as catalyst supports showed higher activity for O_2 reduction than perovskite supports without the macrocycle in alkaline solution. The activity is much less than that of CoTsPc adsorbed on a high-area carbon under similar conditions.
- Most of the high-area carbons used as support materials for catalysts for O_2 reduction are generally unstable at the more positive potentials involved in O_2 generation. Efforts were made to find more stable carbon supports. Several different carbon supports, including both oxidized and non-oxidized Shawinigan black, LBL carbon, graphitized carbon and mildly fluorinated carbon black, were examined at CWRU for use with lead ruthenate pyrochlore. All of these carbons gave similar performance. This is promising because it shows that highly oxidation resistant carbons can be used without sacrificing cathode performance.

The details of this research are given in the annual reports prepared by CWRU for the LBL as well as in published research papers under this project.

II. COMPREHENSIVE SUMMARY OF THE RESEARCH DURING THE PAST YEAR

1. Objectives

The objectives of the research were:

1. to develop a better understanding of the factors controlling O_2 reduction and generation on various electrocatalysts, including transition metal macrocycles and oxides;
2. to use this understanding to identify and develop much higher activity catalysts, both monofunction and bifunction;
3. to establish how catalytic activity for a given O_2 electrocatalyst depends on catalyst-support interactions and to identify stable catalyst supports for bifunctional electrodes.

2. Introduction

Over the past three decades a large research effort has been carried out internationally on a wide range of catalysts for O_2 reduction in alkaline and acid electrolytes and to a lesser extent on O_2 generation, particularly in alkaline electrolyes. Much of this prior research by various groups was "semi-Edisonian" and lacked an adequate understanding of the electronic and steric factors controlling the activity. Consequently, the emphasis on O_2 electrocatalysis research at CWRU is to achieve a better understanding of both O_2 reduction and generation in relation to the basic properties of the catalyst-electrolyte interface. The research also is concerned with the failure mode of these catalysts.

Research during the past year (1 May to 30 April 1992) at CWRU involved work principally on the following aspects of the catalyst systems.

1. Transition Metal Macrocycle Catalysts
   - 1.1 *In Situ* FTIRRAS studies of FeTsPc on Ag
   - 1.2 STM and AFM studies of macrocycles on surfaces.

1.3 Solution-phase voltammetry of the tetrasulfonated phthalocyanines in aprotic organic solvents.

1.4 Oxygen reduction on OPG, Pt and Au surfaces in DMSO with and without CoTsPc in solution.

1.5 Effects of adsorbed tetrasulfonated phthalocyanines on the redox behavior of charged and uncharged species in aqueous electrolytes.

1.6 Effect of methanol and other alcohols on the O_2 reduction electrocatalytic activity of macrocycles in acid and alkaline solutions.

2. Transition Metal Oxides as Catalyst and Support

2.1 O_2 reduction and generation on pyrochlore-based gas-fed electrodes in acid electrolyte.

2.2 Transition metal oxides as support materials for O_2 reduction electrocatalysts.

Appendices A and B summarize the catalyst systems which have significant activity for O_2 reduction and generation, as well as peroxide decomposition, respectively.

1. Transition Metal Macrocycle Catalysts

1.1 *In Situ* FTIRRAS Studies of FeTsPc on Ag.

The iron tetrasulfonated phthalocyanine (FeTsPc) complex adsorbed on an electrode surface at mono- or submonolayer levels has high activity for the 4-electron reduction of O_2 to OH^- in alkaline solutions. The orientation of the complex on the surface has a strong effect on the activity as well as pathway for O_2 reduction. *In-situ* surface-enhanced Raman scattering (SERS) measurements obtained earlier on Ag showed stretching modes involving C=C and C=N bonds of

the macrocycle and provided evidence that the plane of the adsorbed TsPc complex is oriented at an angle to the surface (1). Selection rules, however, are open to question for SERS.

During the past year *in situ* infrared measurements, FTIRRAS, were conducted to obtain structural information for mono- or submonolayers of adsorbed FeTsPc on Ag. Enhanced sensitivity was achieved by using a Dove prism (CaF_2) as a window, instead of a flat window. Dove prisms provide higher incidence angles. First, cyclic voltammetry of Ag electrode in 0.1 M $HClO_4$ containing 10^{-4} M FeTsPc was obtained using the optical cell with the electrode pulled back from the window. The FeTsPc solution was then removed and the cell was filled with a fresh solution of $HClO_4$, without macrocycle, leaving the adsorbed macrocycle on the surface. The Ag electrode was moved close to the optical window at +0.1 V vs. SCE. The potential was switched between +0.1 V and -0.4 V vs. SCE. At each potential 200 scans were made. The above process was repeated until a satisfactory signal-to-noise ratio was achieved (10,000 scans). Spectra at different potentials were obtained which have several derivative peaks corresponding to C=C or C-N vibration modes. In view of the IR selection rules, this provides further evidence that the TsPc is oriented at an angle to the surface and is not completely parallel to the surface.

1.2 STM and AFM Studies of Macrocycles

Considerable information was obtained on the orientation of Fe- and CoTsPc on Ag and other substrates using surface-enhanced Raman and resonant Raman, uv-vis reflectance, and FT infrared reflectance absorption spectroscopies with adsorbed mono- or submonolayer coverages. During the last year, research

was focused on the structural features of the adsorbed phthalocyanines using STM (*ex situ* and *in situ)* and AFM (*ex situ*).

1.2.1 STM Studies

The CoTsPc was preadsorbed on HOPG surface by dipping the HOPG disk at open circuit into an air-saturated aqueous solution of CoTsPc (~1 x 10^{-5} M) (parallel to the liquid surface) for ~20 min. The disk was then removed, washed with pure water and dried in a vacuum oven. *Ex situ* STM measurements with a Pt-Ir tip showed that the plane of the complex is tilted from the perpendicular to the surface. The complexes are parallel to each other but the adjacent complexes are slipped parallel to each other so as to provide for inclination of the central transition metal ion with the pyrrole or bridging nitrogen of the phthalocyanine. However, the ordered layer was distorted by scanning with the STM tip. It is probably caused by the interaction force between the tip and the adsorbed molecules which is reported to be about 10^{-6} N for a few nA tunneling current in vacuum or air.

By operating the STM in a liquid environment, the interaction force between the STM tip and the adorbed molecules is expected to be reduced by 10 or 100 times because of the difference in the dielectric coefficient of the liquid and air. The orientation of the adsorbed layer of CoTsPc on a HOPG surface was, therefore, studied with *in situ* STM in 0.05 M H_2SO_4 under potential control. Pt tips covered with glass were used. The tip potential was controlled to maintain a constant tunneling current. With a modified microcell and Pt wires as reference and counter electrodes, cyclic voltammetry showed the submonolayer adsorption of CoTsPc on the HOPG surface. The *in situ* STM images showed an orientation of the adsorbed complex on HOPG similar to that observed initially with *ex situ*

STM. When the potential was set to the O_2 reduction region, the *in situ* STM images were distorted and reappeared again when the potential was set to the double layer region.

1.2.2 AFM Studies

The molecular orientation of pre-adsorbed CoTsPc on a HOPG surface was also studied with the Nanoscope II AFM in air. The preparation of the preadsorbed layer of CoTsPc on HOPG was described above. The adsorbed layer was characterized by cyclic voltammetry. Si_3N_4 microcantilevers with integrated pyramidel tips were used. The cantilever arm was 100 microns long with a force constant of 0.58 N/m. The AFM tips were checked on freshly cleaned HOPG surface. If the tip gives near atomic resolution on an HOPG surface, it can be used for the studies of molecular orientation of CoTsPc on the surface.

A set of AFM topographies of CoTsPc submonolayer adsorbed on HOPG surface was obtained at a constant force of 2×10^{-8} N. A large scan area (300 x 300 nm) showed ordered molecular structures of CoTsPc. With higher magnification (30 x 30 nm), the images showed an orientation similar to that obtained by *in situ* STM images. Rotation of the sample resulted in the expected changes of the molecular orientation.

The sheet-type polymeric phthalocyanines are of special interest for understanding the 4-electron reduction of O_2 to OH^- on FePc and its modified forms such as FeTsPc and FeTPyPz in alkaline solutions. The sheet-like polymer structures were first prepared and proposed by Drinkard and Bailer based on elemental analysis and titrimetric equivalent weights (2). The concentration of the peripheral carboxylic acid groups was determined by neutralizing the acid groups by standardized NaOH and back titration with standardized HCl. The equivalent

weights were calculated for the various possible oligomers. Achar et al. later reported a method (3) to prepare tetramer phthalocyanines as in Figure 1. However, prior to the present study, there was no direct evidence for the existence of a sheet-type molecular arrangement, except from elemental analysis and titrimetric equivalent weight which are not very definitive.

CoPc oligomers which are coated on an OPG surface, were studied by AFM in this laboratory. The oligomer was coated on the OPG surface by placing 50 μL of 10^{-5} M solution of the polymer in DMSO on the graphite substrate and drying it in a vacuum oven overnight. Crystallites with particle sizes of 30-60 nm were observed by AFM. The profiles of the AFM images showed particles with a step height ~5Å, suggesting that the molecules are stacked parallel to each other and parallel to the graphite surface. Zooming the scanning probe on the top layer of the crystal, one can observe a sheet-shaped molecular structure (Fig. 2). A two-dimensional Fourier transform (2 DFT) of the image given in Figure 2 generates a spectrum with four bright spots with nearly equal distance from the origin. A clear molecular structure is reconstructed by an inverse Fourier transform using the frequencies represented by the four bright spots (Fig. 3). The distance between the two neighboring metal centers is 11 Å and the diameter of the cavity formed between four monomer lobes is 8.4 Å, which agree well with the theoretical values of 10.7 Å and 8.3 Å, respectively, using a molecular modelling program.

1.3 Solution-Phase Voltammetry of Tetrasulfonated Phthalocyanines in Organic Solvents

Earlier studies at CWRU showed that the cyclic voltammetry of Co- and FeTsPc on OPG disk electrodes in aqueous acid or alkaline electrolytes corresponds to the redox processes of the adsorbed macrocycle species and not the

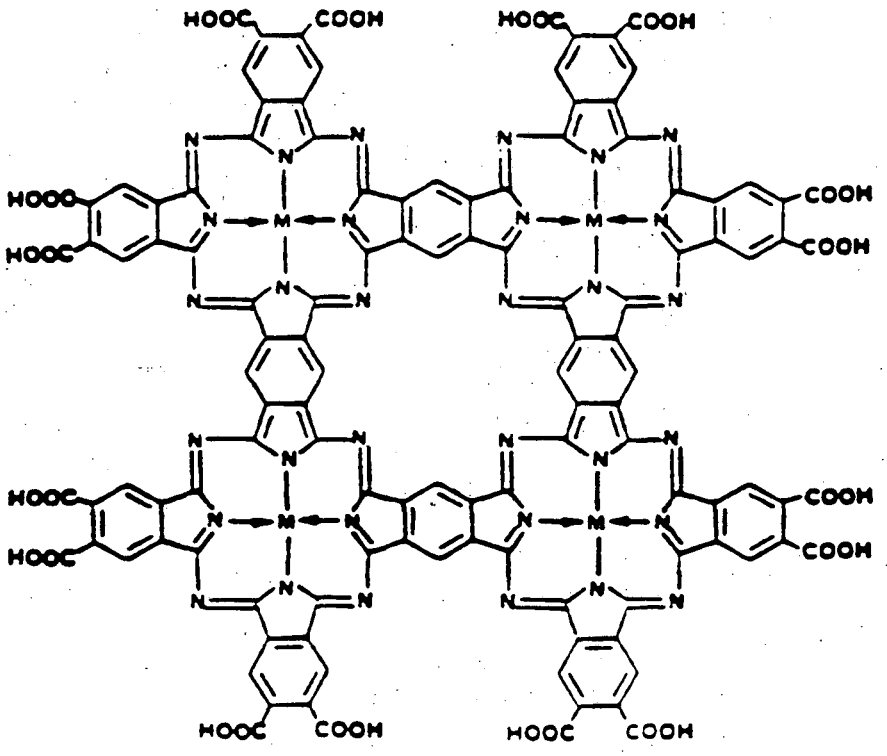

Fig. 1. Polymeric phthalocyanine (fused type, fragment)

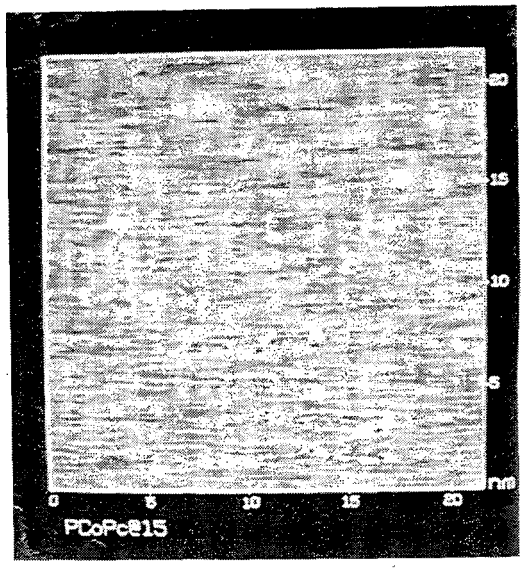

Fig. 2. AFM image of the CoPc oligomer which was obtained by zooming the scanning probe on top of the crystal.

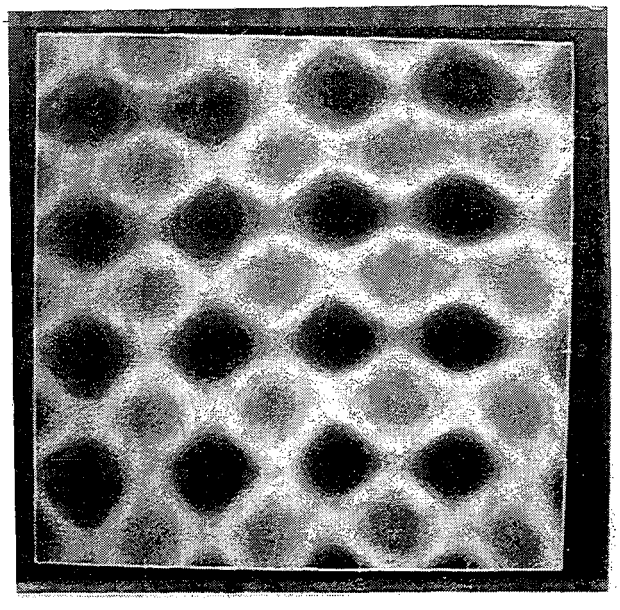

Fig. 3. A molecular structure of CoPc oligomer that was generated by computer using an inverse Fourier transform from Fig. 2.

dissolved species in solution (4). Iron pyridino-porphyrazine (FeTPyPz), a phthalocyanine similar to FeTsPc, also does not show voltammetric peaks in aqueous acid electrolyte associated with the outer-sphere heterogeneous electron transfer (5). FeTPyPz has appreciable solubility in acid solutions, and under this condition most of the pyridino groups are expected to be protonated. Both the solution-phase and adsorbed FeTPyPz would be positively charged and repulse each other, thus suppressing the outer-sphere electron transfer kinetics. The interaction of the adsorbed macrocycle with the substrate is expected to cause a substantial difference in the redox behavior of the dissolved and the adsorbed species.

To separate the redox peaks associated with the non-adsorbed species from those for the adsorbed species on the electrode surface, voltammetric studies of these macrocycles were carried out in different solvents. Voltammetric measurements of CoTsPc in CH_3CN and $(CH_3)_2SO$ containing tetraethyl ammonium perchlorate as the supporting electrolyte were obtained on OPG, Au and Pt disk electrodes. Pure water was added to CH_3CN in the ratio 1 H_2O/5CH_3CN, and with CoTsPc at a concentration of ~1 x 10^{-4} M. The macrocycle is sparingly soluble in pure CH_3CN. The acetonitrile (Aldrich, anhydrous, 99+%, water <0.005%) and dimethyl sulfoxide (Fischer, reagent grade, water <0.04%) were further dried in a column of 4 Å molecular sieve and then stored over the molecular sieve (Aldrich) for at least 24 h prior to use. Tetraethyl ammonium perchlorate (Fluka, 99%) which was used as the supporting electrolyte was dried in a vacuum oven at 60°C for at least 48 h.

Three quasi-reversible redox peaks of the solution-phase species of CoTsPc were obtained in non-aqueous solutions on all three electrodes. There are

no significant differences in the peak potentials for the three electrodes in the same organic solvent (Table I). The currents associated with the voltammetric peaks in aprotic organic solvents are low (of the order of a few $\mu A/cm^2$ at a sweep rate of 150 mV/s and concentration of ~1 x 10^{-4} M). One explanation for this behavior may be that the macrocycle is highly associated in the organic solvents. This can lead to various complications which result in smaller and broader redox peaks. The heights of the peak depend on convection in the solution and are a linear function of the square root of the scan rate. These tests indicate that the redox peaks in the organic solvent correspond to the dissolved species of CoTsPc. Further, the peak potentials with CoTsPc and CoPc in $(CH_3)_2SO$ are almost similar. This is probably due to the fact that the SO_3H groups are not ionized in the organic solvent. Recently we have observed the outer-sphere electron transfer reaction for TsPc's on a tin-doped indium oxide (ITO) electrode in 0.05 M H_2SO_4. These macrocycles are not adsorbed on this electrode surface in 0.05 M H_2SO_4. The pH dependence of this reaction on ITO is under investigation.

An explanation for the absence of voltammetric peaks of these macrocycles in aqueous solution is based on the excess negative charge associated with the TsPc ligand in solution because of the ionized SO_3^- groups attached to the four aromatic rings. Another explanation involves the adsorption of the macrocycle edge-on on the electrode surface, where the distance between the electrode surface and the solution-phase macrocycle molecule at the point of closest approach may be ~15Å. This large distance may impede the electron tunneling between the solution-phase macrocycle and the adsorbed species on the electrode. Resonance tunneling might be involved, in which case tunneling may occur over a large distance.

TABLE I

Solution-phase Voltammetric Redox Potentials of CoTsPc (~1 x 10^{-4} M) in 5:1 Mixture* of CH_3CN and H_2O (de-aerated) on Various Electrodes

Electrolyte: 0.1 M Tetraethyl ammonium perchlorate
Scan Rate: 150 mV/s
Peak Potentials (V) vs SCE

Electrode	Peak 1	Peak 2	Peak 3
Pt	—	-0.40[c]	+0.42[c]
	—	-0.20[a]	+0.53[a]
Au	—	-0.38[c]	+0.42[c]
	—	-0.20[a]	+0.54[a]
OPG	-1.24[c]	-0.38[c]	+0.43[c]
	-1.10[a]	-0.22[a]	+0.54[a]

*CoTsPc is not completely soluble in pure CH_3CN
[a]anodic peak potential
[c]cathodic peak potential
Peak 1 corresponds to the reduction of the TsPc ligand
Peak 2 corresponds to the reduction of Co (II) to Co (I)
Peak 3 corresponds to the reduction of Co (III) to Co (II)

1.4 Oxygen Reduction on OPG, Pt and Au Surfaces in Dimethyl Sulfoxide with and without CoTsPc in Solution.

Oxygen is reduced by a 2-electron pathway to peroxide on OPG and polycrystalline Au surfaces in alkaline aqueous solution. However, clean Pt and Au (100) catalyze the 4-electron reduction of O_2 to OH^- under similar conditions. To obtain a better understanding of the mechanistic aspects of O_2 reduction, the reduction of O_2 on OPG, Au and Pt surfaces was examined in an aprotic non-aqueous solvent (DMSO) containing TEAP as the supporting electrolyte, with and without the presence of CoTsPc in the solution. CoTsPc is a good catalyst for the 2-electron reduction of O_2 to peroxide in acid and alkaline aqueous solutions. During the past year, O_2 reduction was studied on OPG, Pt and Au surfaces in DMSO using linear sweep voltammetry and the rotating disk electrode (RDE) technique at 25°C.

O_2 reduction on these electrode materials in DMSO showed a quasi-reversible one-electron reduction to superoxide. The cathodic peak potentials in the voltammograms were -0.85 V, -0.89 V and -0.90 V vs. SCE for OPG, and polycrystalline Au and Pt respectively. This indicates that the rate of electron transfer in aprotic media depends on the electrode material, in agreement with earlier results (6-8). The separation of the cathodic and anodic peak potentials for OPG (ΔV= 0.16 V) is less than those for Au (ΔV = 0.22 V) and Pt (ΔV = 0.20 V), respectively. The addition of CoTsPc (~5 x 10^{-5} M) to the solution reduces the peak heights to some extent. There is an increase in the separation of the peak potentials with all of the electrodes, except for OPG in which case there is a slight decrease in the separation of the cathodic and anodic peak potentials. The results

show no significant changes in the O_2 reduction reaction in DMSO which contain CoTsPc.

The curves for O_2 reduction on rotating disk electrode in DMSO containing 0.1 M TEAP as the supporting electrolyte are given in Figures 4-6. The half-wave potential ($E_{1/2}$) is ~85 mV more positive for OPG than for Au and ~25 mV more positive for Au than for Pt. The plots of limiting current densities (i_L) vs. square root of rotation rates ($f^{1/2}$) show that i_L is approximately equal to the diffusion limiting current density i_D (A/cm^2) (Fig. 7). The observed B values from the Levich plots are 6.1×10^{-5} for OPG, 6.3×10^{-5} for Au and 6.4×10^{-5} A cm^{-2} $rpm^{-1/2}$ for Pt respectively. These values agree fairly well with the calculated value of 7.1×10^{-5} A cm^{-2} $rpm^{-1/2}$ for n = 1 and from the other data (7,9,10) (see Fig. 7). The i^{-1} vs. $f^{-1/2}$ plots show that the slope increases at less negative potentials on all of the surfaces, indicating the relative influence of the back reaction. The mass-transport-corrected Tafel plots for the forward (positive to negative) potential sweep for OPG, Au and Pt are shown in Figure 8. The Tafel slopes are -144 mV/decade for OPG, -231 mV/decade for Au and -227 mV/decade for Pt and the transfer coefficients are 0.41 for OPG and 0.26 for Au or Pt, respectively. The differences between these parameters for OPG and Au or Pt electrodes may be due to differences in the true surface area, functional groups on the OPG surface, and the point of zero charge (PZC) of these materials.

The RDE studies also show no major changes in the O_2 reduction reaction in DMSO containing CoTsPc. The Au and Pt electrodes show some inhibition for the electrode reaction ($O_2 + e^- \rightarrow O_2^-$) in the presence of CoTsPc. The $E_{1/2}$ values for Au and Pt are ~75 mV and ~40 mV more negative, respectively, with CoTsPc in solution. However, the OPG electrode shows negligible effect under similar

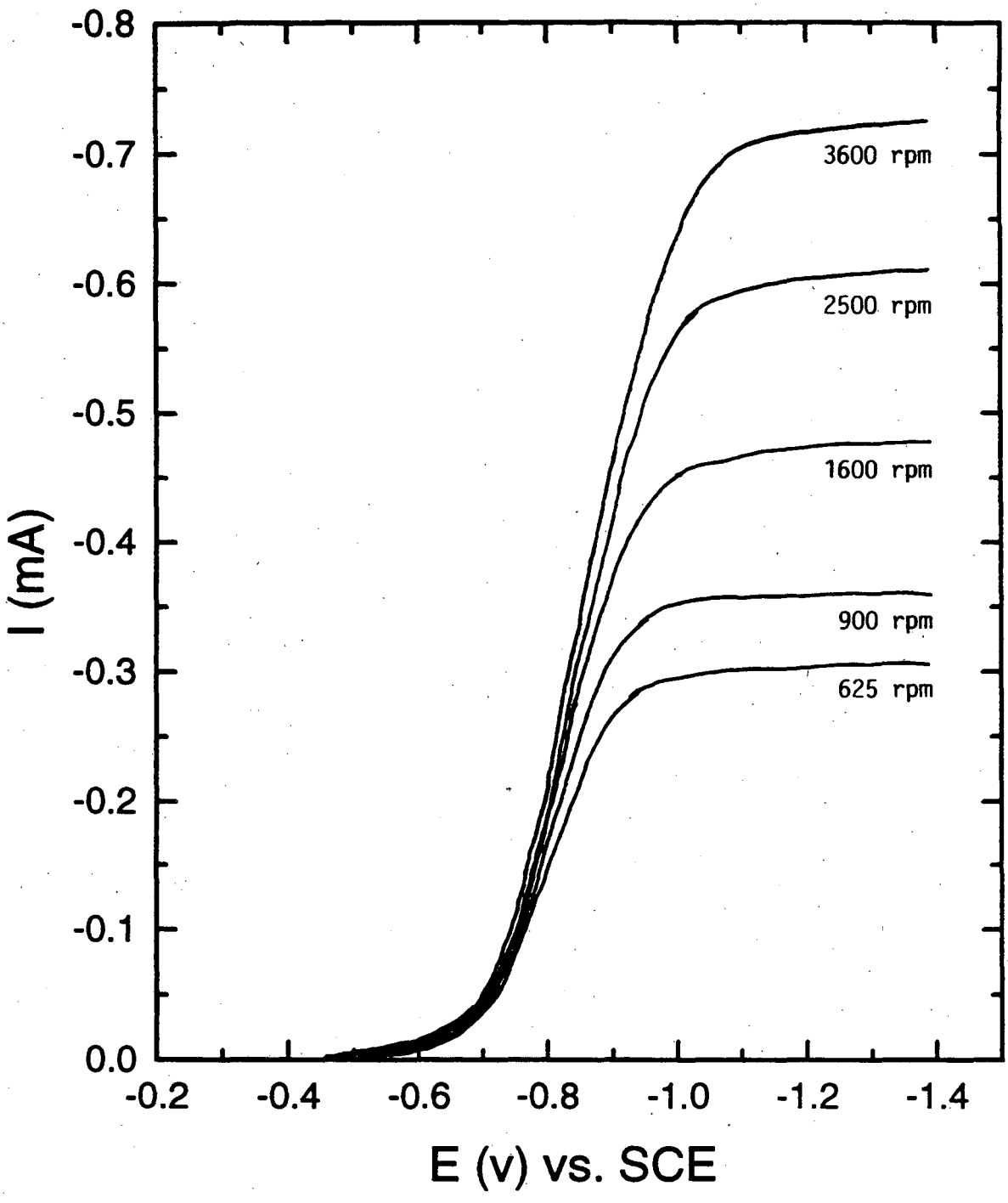

Fig. 4. Disk currents for O_2 reduction on OPG in O_2-saturated DMSO (0.1 M TEAP).

Sweep rate = 20 mV/s.
Electrode area = 0.2 cm^2.
Temperature = 25°C.

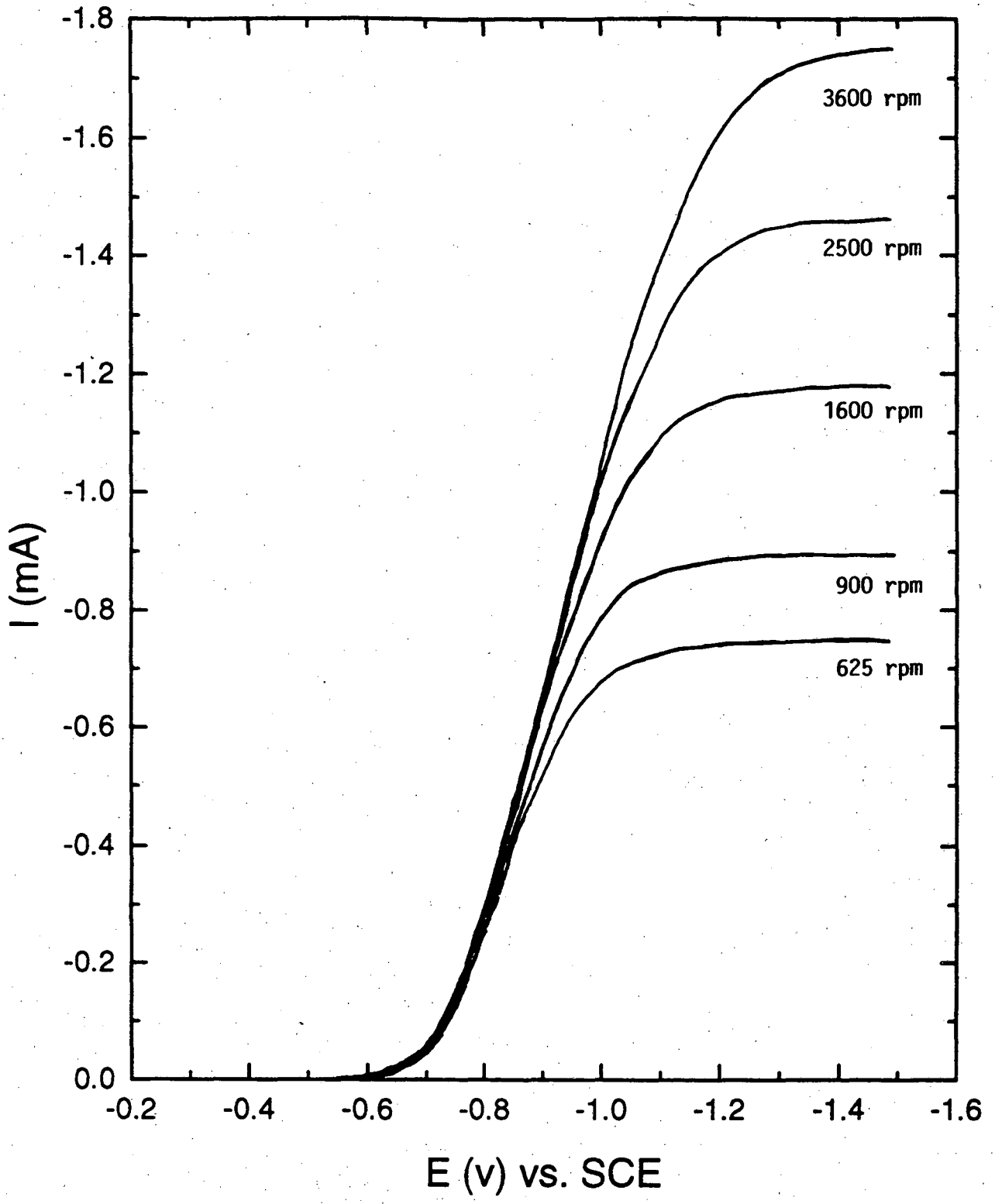

Fig. 5. Disk currents for O_2 reduction on polycrystalline Au in O_2-saturated DMSO (0.1 MTEAP).

Sweep rate = 20 mV/s.
Electrode area = 0.46 cm^2.
Temperature = 25 °C.

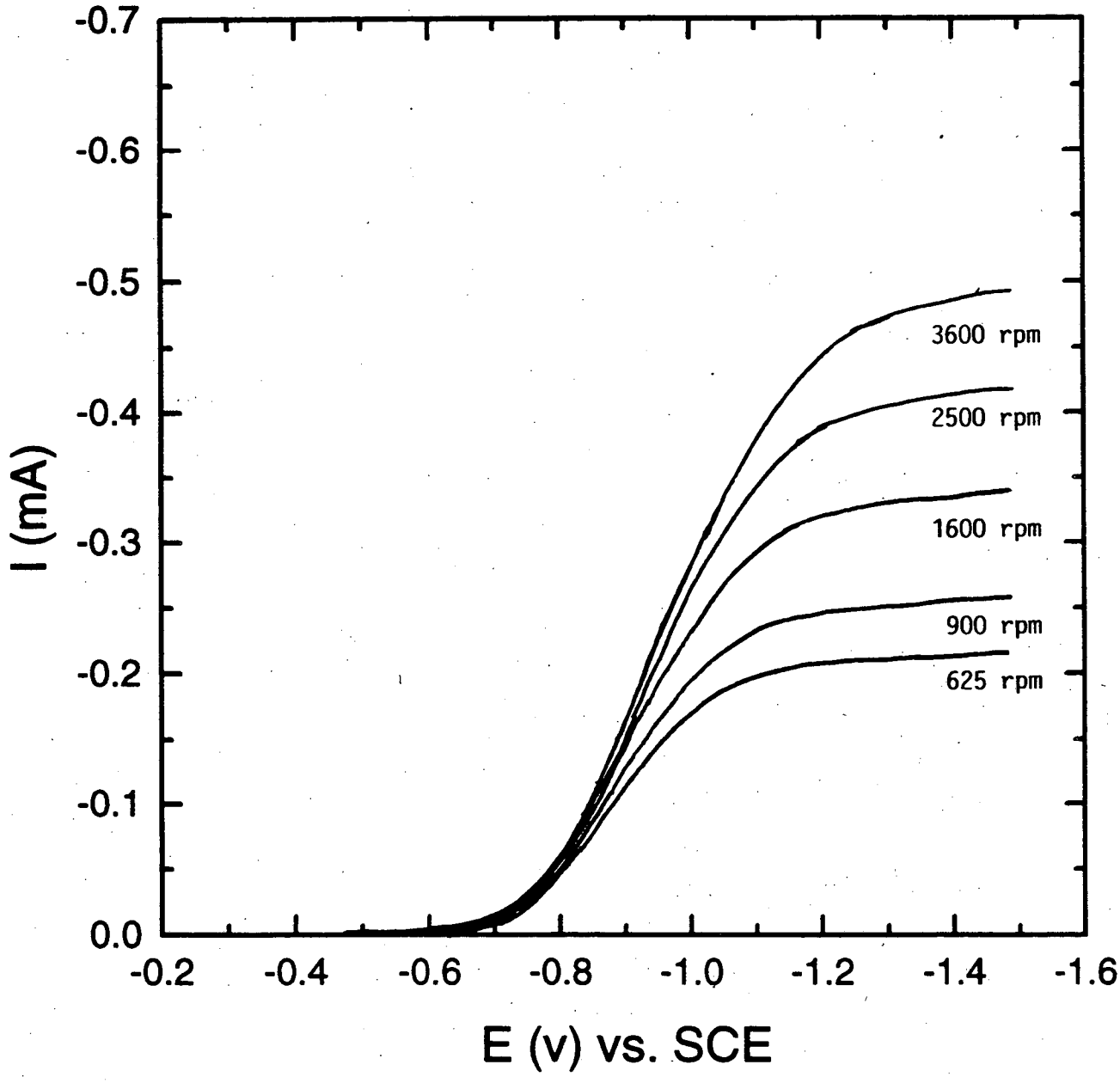

Fig. 6. Disk currents for O_2 reduction on polycrystalline Pt in O_2-saturated DMSO (0.1 MTEAP).

Sweep rate = 20 mV/s.
Electrode area = 0.125 cm^2.
Temperature = 25 ^oC.

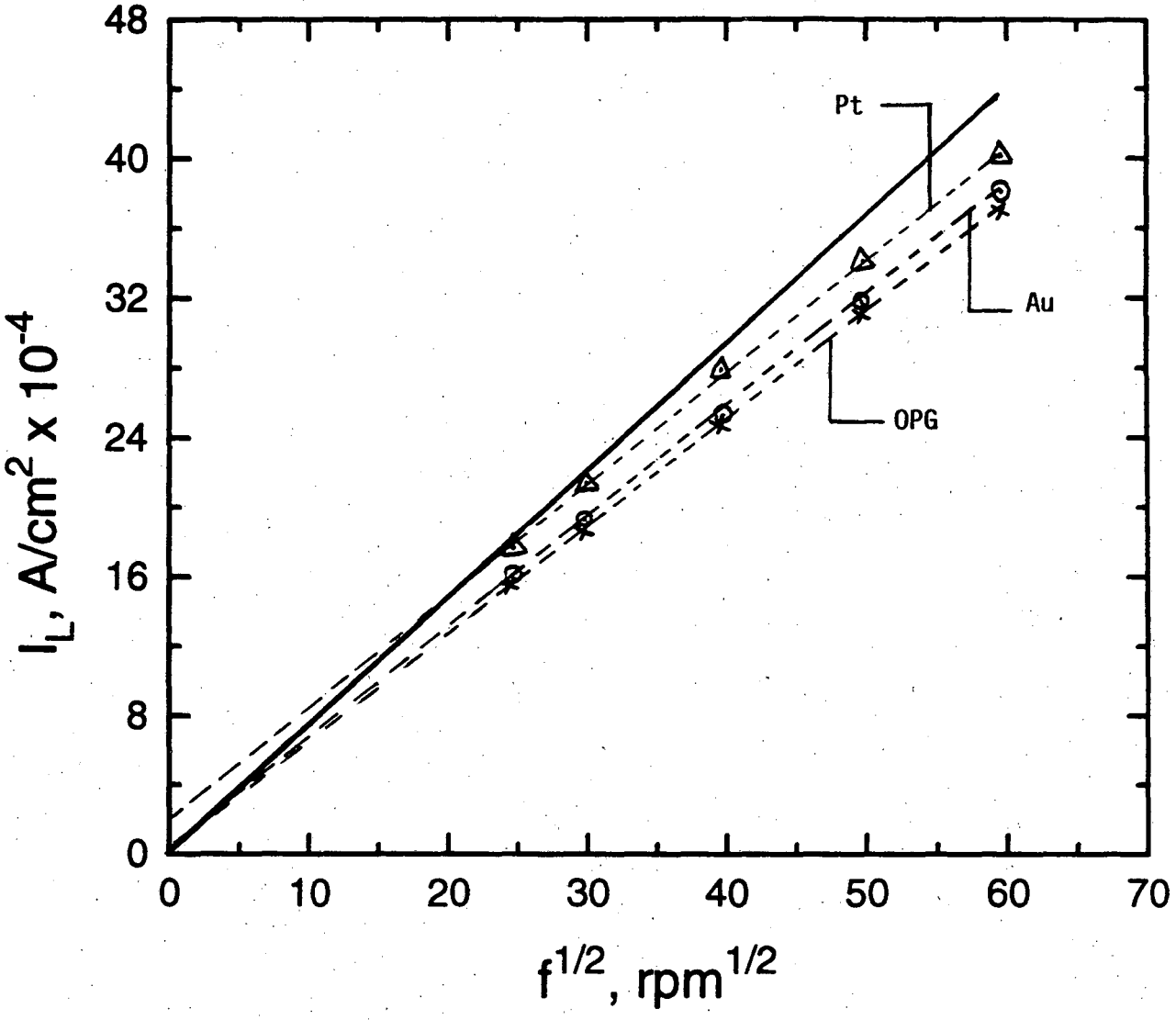

Fig. 7. Levich plots for O_2 reduction in DMSO (0.1 M TEAP) on OPG (x), Au (o) and Pt (Δ) based on Figs. 4, 5 and 6 respectively. Current values were measured at -1.4 V for OPG -1.5 V for Au and -1.6 V vs. SCE for Pt. Solid line calculated from the literature values of D_{O_2}, ν and C_{O_2} for n = 1. Temperature = 25°C

D_{O_2}= 2.82 x 10^{-5} cm^2 s^{-1}(9)
ν = 1.79 x 10^{-2} cm^2 s^{-1}(10)
C_{O_2}= 2.1 x 10^{-6} mol cm^{-3}(7)

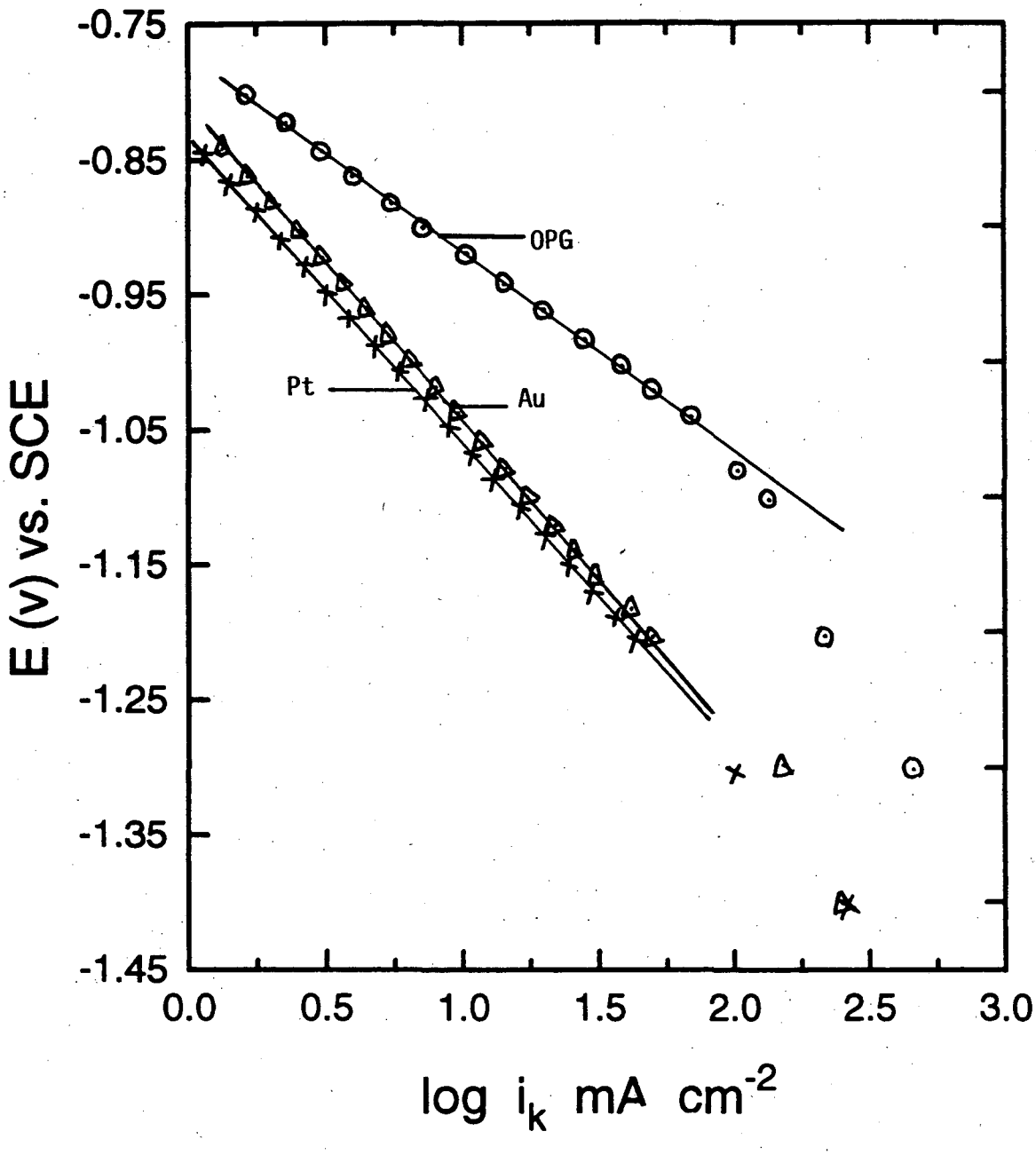

Fig. 8. Mass-transport-corrected Tafel plots for O_2 reduction in O_2-saturated DMSO (0.1 M TEAP) on OPG (o), Au(Δ) and Pt (x) for forward scan. Data taken from figs. 4, 5 and 6, respectively, for 2500 rpm. Temperature = 25°C.

conditions (~10 mV more negative value of $E_{1/2}$) with CoTsPc in solution. These results confirm that the rate of the electron transfer for O_2 reduction in an aprotic media depends on the electrode material. The addition of CoTsPc to the DMSO solution with 0.1 M TEAP as the supporting electrolyte causes only a small change in the rate constant (see Tables II and III).

The standard rate constants for the reaction $O_2 + e^- \rightarrow O_2^-$ on various surfaces, with and without the CoTsPc, are calculated from voltammetric studies (11) and are recorded in Tables II and III along with other parameters. The values of the standard heterogeneous electron transfer rate constants (k^o) calculated from voltammetry and rotating disk electrode techniques agree fairly well.

1.5. Effects of Adsorbed Tetrasulfonated Phthalocyanines on the Redox Behavior of Charged and Uncharged Species in Aqueous Electrolytes

Cobalt and iron tetrasulfonated phthalocyanines adsorbed on OPG disk electrode at mono- or submonolayer coverages, were found to be good electrocatalysts for O_2 reduction in aqueous alkaline and acid electrolytes. Earlier studies at CWRU showed that the solution-phase cyclic voltammetry of Co and FeTsPc in aqueous acid or alkaline electrolytes on OPG corresponds to the redox processes of the adsorbed macrocycle species and not the dissolved species in solution (4). However, the solution-phase redox peaks for these macrocycles on OPG, Au and Pt electrodes were recently observed in organic solvents such as $(CH_3)_2SO$ with tetraethyl ammonium perchlorate (TAEP) as the supporting electrolyte. An explanation for the absence of the solution-phase peaks of the macrocycle was based on the excess negative charge associated with the TsPc ligand in aqueous solution as a result of the ionized SO_3^- groups attached to the four aromatic rings. Another explanation may be related to the edge-on adsorption

TABLE II

Standard Electrode Reaction Rate Constants k^0 for O_2 Reduction on OPG, Au and Pt in Dimethyl Sulfoxide (0.1 M TEAP) with CoTsPc in the Solution (~1 x 10^{-4} M) at 25°C

Electrode Materials	Scan Rate ($mV\ s^{-1}$)	ΔEp (mV)	$\Psi^{a,b}$	k^0 ($cm\ s^{-1}$)	Average k^0 ($cm\ s^{-1}$)
OPG	150	160	0.190	0.0029	0.003
($\alpha = 0.38$)	100	150	0.220	0.0028	
	50	130	0.300	0.0027	
	20	100	0.580	0.0033	
	10	90	0.810	0.0033	
Au	150	275	0.065	0.0012	0.0012
($\alpha = 0.21$)	100	250	0.065	0.001	
	50	205	0.110	0.0012	
	20	160	0.190	0.0013	
	10	140	0.250	0.0012	
Pt	150	310	0.065	0.0011	0.0009
($\alpha = 0.25$)	100	285	0.065	0.0009	
	50	230	0.080	0.0008	
	20	185	0.140	0.0009	
	10	158	0.200	0.0009	

[a]Determined by interpolation from values in Table 1 of reference 11

[b]Sweep direction, positive to negative

αTransfer coefficient

ΨA function of the anodic - cathodic peak potential separation and is tabulated in Ref. 11

TABLE III

Standard Electrode Reaction Rate Constants k^0 for O_2 Reduction on OPG, Au and Pt in Dimethyl Sulfoxide (0.1 M TEAP) without CoTsPc in the Solution (~1 x 10^{-4} M) at 25°C

Electrode Materials	Scan Rate (mV s^{-1})	ΔEp (mV)	$\Psi^{a,b}$	k^0 x 10^{-2} (cm s^{-1})	Average k^0 x 10^{-2}
OPG	150	185	0.130	0.19	0.23
(α = 0.41)	100	165	0.180	0.22	
	50	140	0.250	0.22	
	20	110	0.445	0.24	
	10	95	0.680	0.26	
Au	150	260	0.065	0.11	0.13
(α = 0.26)	100	225	0.085	0.12	
	50	185	0.140	0.14	
	20	145	0.235	0.15	
	10	125	0.330	0.15	
Pt	150	280	0.065	0.11	0.12
(α = 0.26)	100	240	0.070	0.10	
	50	200	0.118	0.12	
	20	150	0.220	0.14	
	10	130	0.300	0.14	

[a]Determined by interpolation from values in Table 1 of reference 11
[b]Sweep direction, positive to negative
αTransfer coefficient
ΨA function of the anodic - cathodic peak potential separation (see Table II)

of the macrocycle on the electrode surface. In this case the distance between the electrode surface and the solution-phase macrocycle molecules at the point of closest approach may be ~15Å. This large distance may impede electron tunneling between the solution-phase macrocycle and the adsorbed species on the electrode. Resonance tunneling might be involved, in which case tunneling may occur over a larger distance.

To examine further the heterogeneous redox processes of the TsPc's in aqueous electrolytes, the effects of preadsorbed tetrasulfonated phthalocyanines on OPG or in solution (~1 x 10^{-4} M) was investigated using linear sweep voltammetry. This has involved the redox behavior of negatively charged $K_3Fe(CN)_6$ and $K_4Fe(CN)_6$, uncharged o-tolidine and positively charged $Fe(ClO_4)_3$ in aqueous acid and alkaline solutions. Various tetrasulfonated phthalocyanines were used, including CoTsPc, FeTsPc, CuTsPc and H_2TsPc.

In general, the redox behavior for $K_3Fe(CN)_6$ and $K_4Fe(CN)_6$ or their 1:1 mixture (1 x 10^{-3} M) on OPG electrodes with preadsorbed macrocycle becomes less reversible (more separation of the voltammetric cathodic and anodic peak potentials) in acid electrolyte (0.05 M H_2SO_4). There is also a decrease in the magnitude of the cathodic and anodic peaks of the redox species of the pre-adsorbed macrocycle as compared to those for the same electrode without macrocycle present. The irreversibility is further increased and the magnitude of the peak heights decreased if the macrocycle (~1 x 10^{-4} M) is in the solution. A similar redox behavior is obtained for the ferri- and ferro-cyanide in the alkaline solution (0.1 M NaOH) for various macrocycles pre-adsorbed on the OPG or added in the solution except for the CoTsPc. When it is added to the alkaline solution containing ferri- or ferro-cyanide or their mixture, the redox behavior

became more reversible and the peak heights increased. This is probably due to the fact that CoTsPc acts as a mediator for electron transfer because the redox potential of CoTsPc lies in the same potential range as that of the ferri- and ferrocyanide species in alkaline solution.

In comparing the effect of adsorbed CoTsPc on the redox behavior of $K_3Fe(CN)_6$, o-tolidine and $Fe(ClO_4)_3$ (1×10^{-3} M each) in 0.1 M $HClO_4$ solution, it was observed that the separation of the voltammetric anodic and cathodic peak potentials become greater with $K_3Fe(CN)_6$, almost no change with the o-tolidine and less with $Fe(ClO_4)_3$ (Figures 9-11). This double layer effect is more pronounced when CoTsPc (~1×10^{-4} M) is in solution. The results provide evidence that the charge associated with the TsPc ligand in aqueous solution is responsible for the absence of the solution-phase voltammetric peaks for tetrasulfonated phthalocyanines in aqueous electrolytes. Iron pyridino-porphyrazine (FeTPyPz), a phthalocyanine similar to FeTsPc, also does not show voltammetric peaks in aqueous electrolytes (5). In contrast to FeTsPc, however, the FeTPyPz does not have large charge on the ligand.

1.6 Effect of Methanol and Other Alcohols on the O_2 Reduction Electrocatalytic Activity of Macrocycles on OPG in Acid and Alkaline Solutions

Transition metal macrocycles on high-area carbons were found to be good electrocatalysts for O_2 reduction in alkaline solutions. Earlier studies showed the effect of coordinating agents on the redox properties and O_2 reduction electrocatalytic activity of transition metal macrocycles in alkaline solution (12). It is shown that CN^- ions coordinate with specific valency states of the transition metals such as Fe and Co in phthalocyanines and porphyrins, and have a substantial poisoning effect on O_2 reduction.

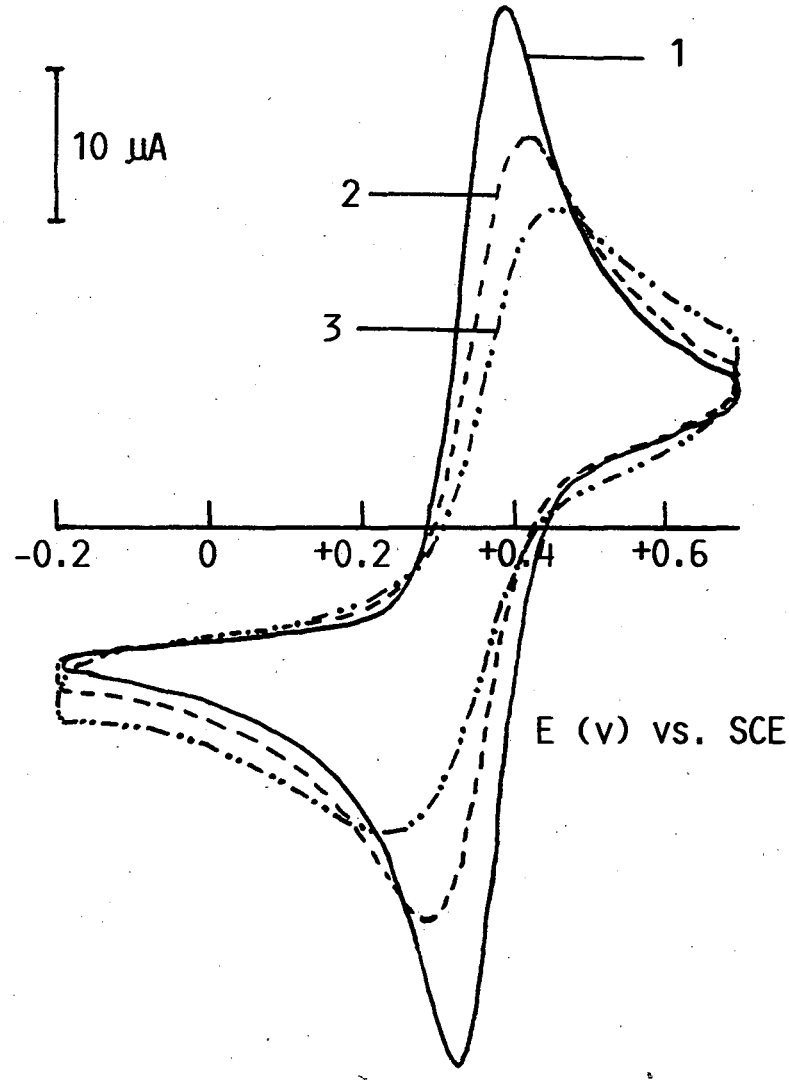

Fig. 9. Cyclic voltammetry of $K_3Fe(CN)_6$ (~1 x 10^{-3} M) in 0.1 M $HClO_4$ (deaerated) in the presence and absence of CoTsPc adsorbed on the electrode surface or in solution at 25°C.

1 - Voltammetric curve for $K_3Fe(CN)_6$ in 0.1 M $HClO_4$ on OPG. No CoTsPc on the surface or in solution.

2 - Voltammetric curve for $K_3Fe(CN)_6$ in 0.1 M $HClO_4$ on CoTsPc preadsorbed on OPG.

3 - Voltammetric curve for $K_3Fe(CN)_6$ in 0.1 M $HClO_4$ on OPG with ~1 x 10^{-3} M CoTsPc in solution.

Area of the electrode = 0.2 cm^2
Scan rate = 100 mV/s

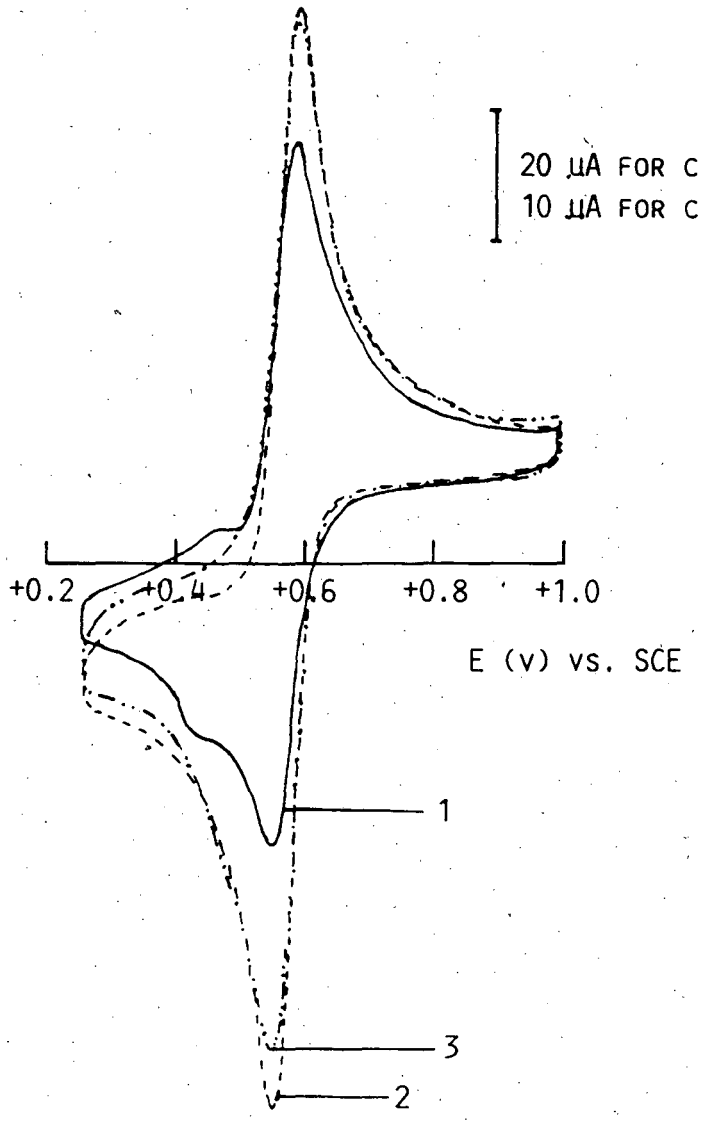

Fig. 10. Cyclic voltammetry of tolidine (~1 x 10^{-3} M) on OPG in 0.1 M $HClO_4$ (deaerated) in the presence and absence of CoTsPc adsorbed on the electrode surface or in solution at 25°C.

1 - Voltammetric curve for tolidine in 0.1 M $HClO_4$ on OPG. No CoTsPc on the surface or in solution.

2 - Voltammetric curve for tolidine in 0.1 M $HClO_4$ on CoTsPc preadsorbed on OPG.

3 - Voltammetric curve for tolidine in 0.1 M $HClO_4$ on OPG with ~1 x 10^{-4} M CoTsPc in solution.

Area of the electrode = 0.2 cm^2
scan rate = 100 mV/s.

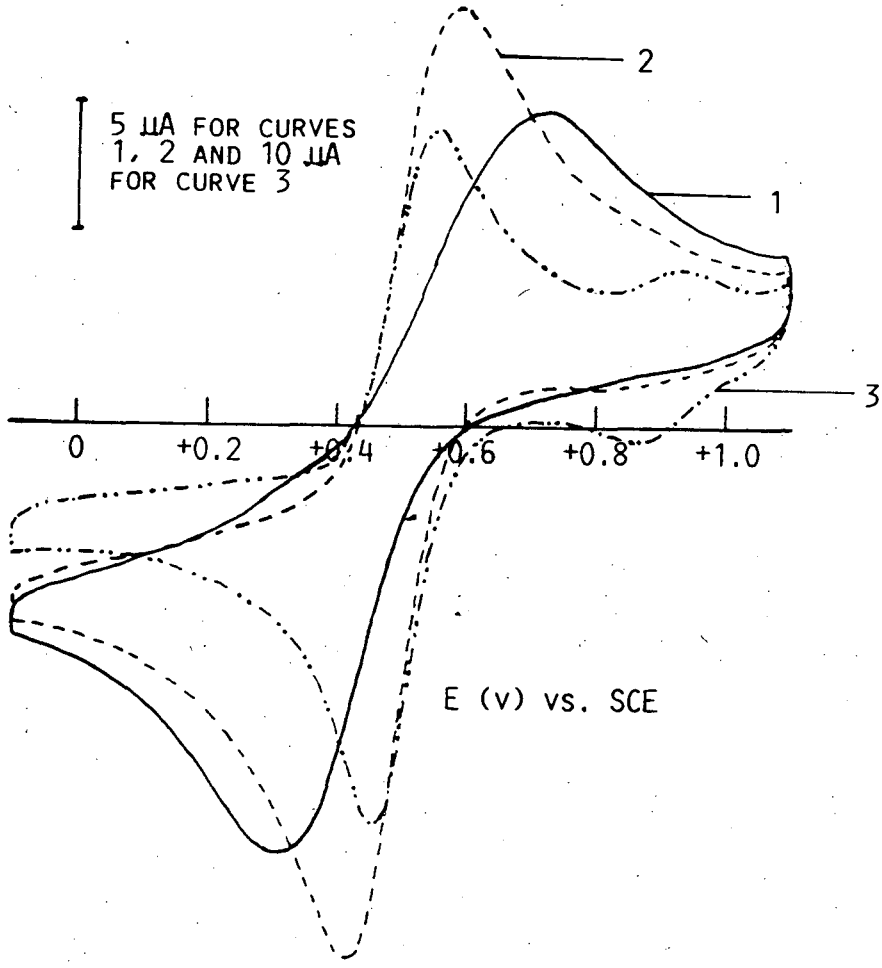

Fig. 11. Cyclic voltammetry of $Fe(ClO_4)_3$ (~1 x 10^{-3} M) on OPG in 0.1 M $HClO_4$ (deaerated) in the presence and absence of CoTsPc adsorbed on the electrode surface or in solution 25°C.

1 - Voltammetric curve for $Fe(ClO_4)_3$ in 0.1 M $HClO_4$ on OPG. No CoTsPc on the surface or in solution.

2 - Voltammetric curve for $Fe(ClO_4)_3$ in 0.1 M $HClO_4$ on CoTsPc preadsorbed on OPG.

3 - Voltammetric curve for $Fe(ClO_4)_3$ in 0.1 M $HClO_4$ on OPG with ~1 x 10^{-4} M CoTsPc in solution.

Area of the electrode = 0.2 cm^2
scan rate = 100 mV/s.

To better understand the redox properties and O_2 reduction electrocatalysis on transition metal macrocycles, the effect of alcohols such as methanol, isobutanol and n-amyl alcohol on the electrochemical properties and O_2 reduction behavior of CoTsPc were examined. These alcohols may change the structure of the interface and orientation of the adsorbed macrocycle on the surface. The effects of methanol and its reaction intermediates on O_2 reduction are also of interest for the identification of methanol-tolerant electrocatalysts for O_2 reduction in methanol-air fuel cells.

The addition of isobutyl alcohol and n-amyl alcohol in alkaline solution (0.1 M NaOH) containing CoTsPc (~2 x 10^{-5} M) on OPG electrodes showed a decrease in the magnitude of the redox peak Co(II)/Co(I) with complete suppression of this peak at ~1 M and 0.4 M concentration of the alcohols, respectively. When this electrode was washed and dipped in a fresh alkaline solution without the macrocycle, the redox peak reappeared at about the same potential, but decreased in magnitude (~33%) as compared to that with no alcohol in solution. No significant suppression of the redox peaks was found with the addition of methanol (≤2 M) in solution. The half-wave potential for O_2 reduction on CoTsPc, (preadsorbed on an OPG disk electrode from alkaline solution (~1 x 10^{-4} M)) in the presence of these alcohols is ~60 mV more positive than O_2 reduction in the absence of these alcohols. This may be due to the increase in the adsorption of the macrocycle on the electrode surface as a result of changes in the dielectric property of the solvent containing alcohols.

O_2-reduction polarization measurements were also carried out in 2.5 M H_2SO_4 at 60°C using porous gas-fed electrodes containing pyrolyzed macrocycles (CoTMPP and CoTAA adsorbed on high area-carbon). The presence of ~1 M

methanol in the solution hardly affected the O_2 reduction performance (Fig. 12). This is quite encouraging for air electrodes in acid electrolyte methanol-air fuel cell.

2. Transition Metal Oxides as Catalyst and Support

2.1 O_2 Reduction and Generation on Pyrochlore-Based Gas-Fed Electrodes in Acid Electrolyte

Metal oxides with the pyrochlore structure, particularly the stoichiometric lead ruthenate, $Pb_2Ru_2O_{7-y}$, were found to be very active catalysts for both O_2 reduction and generation in alkaline solutions with carbon supports or in a self-supporting mode (i.e., without high-area carbon as catalysts support). The lead-ruthenate pyrochlores were examined both as an electrocatalyst and as a support materials to Pt for O_2 reduction and generation in acid electrolyte (2.5 M H_2SO_4 at 60°C) (Fig. 13). A Nafion 117 (DuPont) membrane was pressed on the electrolyte side of the electrode to prevent the dissolution of Pb and Ru from the pyrochlore in the acid solution. The performance for O_2 reduction with the pyrochlore in gas-fed electrodes was found to be significantly lower in acid than in alkaline solution (i.e., over 200 mV more polarization at -10 mA/cm^2). Previous work (13) showed that the reaction order for OH^- was -0.5 over the pH range 12 to 14, but the mechanism changes in going from pH 14 to 1. It was found that the O_2 generation reaction occurred almost as readily in acid as in alkaline solution but with a higher Tafel slope (~80 mV/decade in acid vs. ~40 mV/decade in alkaline solution). The higher Tafel slope is not encouraging because the polarization at higher current densities becomes larger than that for the lower slope.

The O_2 reduction performance was much better with Pt supported on a pyrochlore as compared with a pyrochlore alone. Approximately 10 wt% Pt was

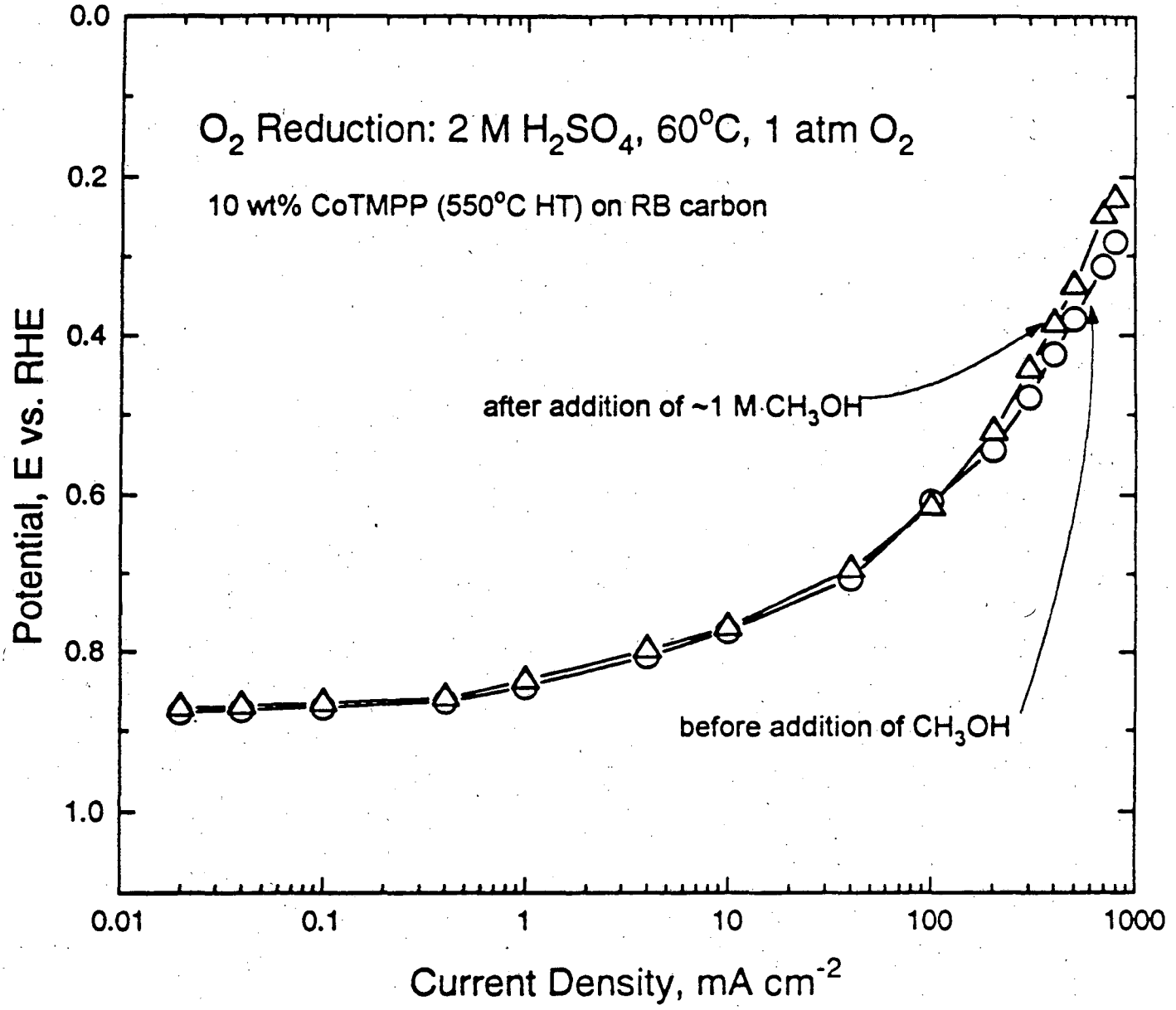

Fig. 12. Steady-state polarization curves (IR-free) for O_2 reduction with porous gas-fed electrodes.

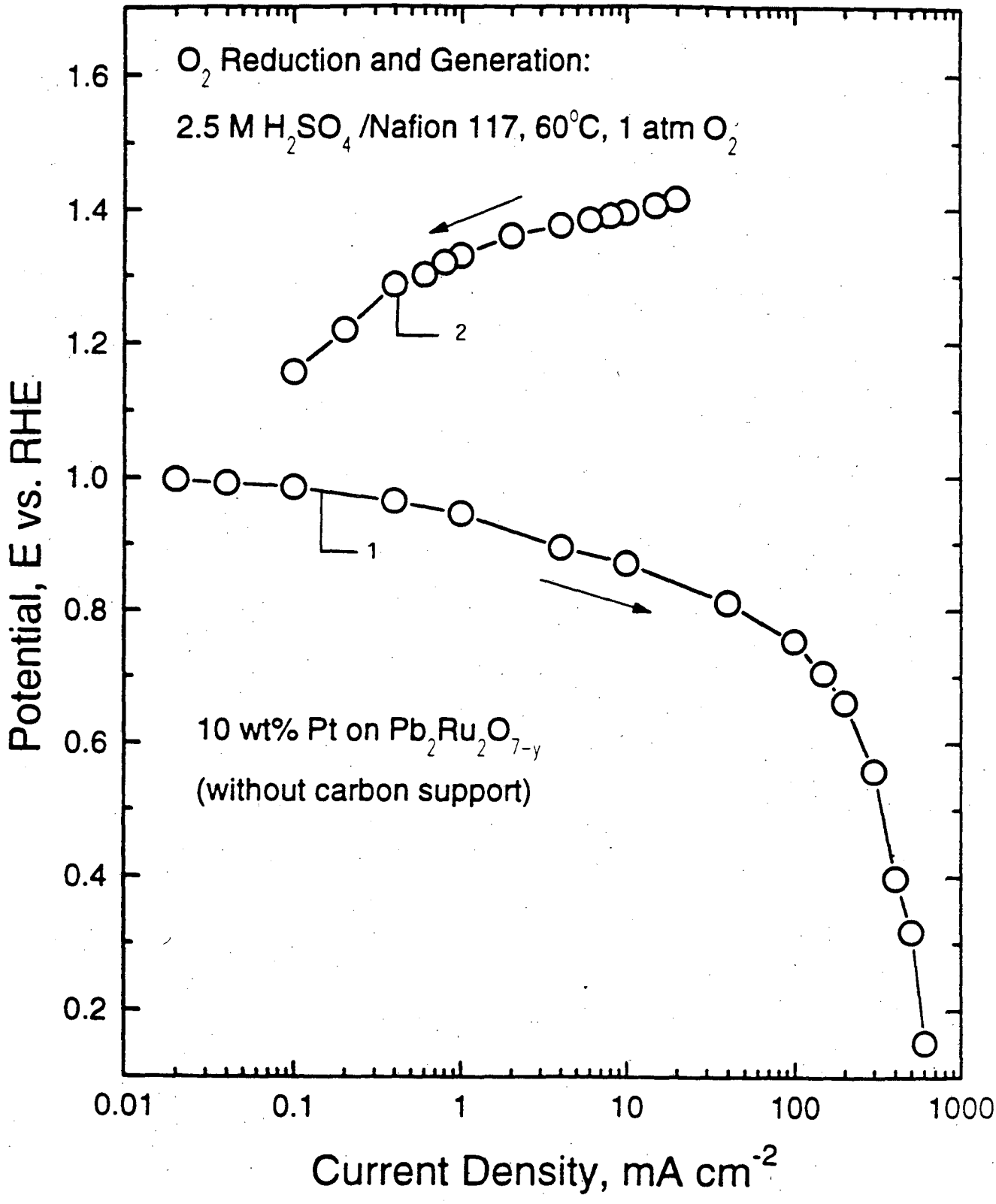

Fig. 13. Steady-state polarization curves (IR-free) for O_2 reduction (1) and generation (2) with porous gas-fed electrodes.

deposited using the Prototech method (14). The O_2 generation performance was also significantly improved (~40 mV/decade Tafel slope) with deposited Pt (Fig. 13). Thus there is some promise for the bifunctional O_2 electrode in acid electrolyte using Pt supported on lead ruthenate pyrochlore.

Measurements of O_2 reduction on gas-fed electrode were also carried out in concentrated KOH (~150°C) using Li-doped NiO as a catalyst support for Pt and Au catalysts. The Pt was deposited on the Li-NiO using the Prototech method, which involves the use of the Pt sulfite complex (15). The Au catalyst was prepared according to a Prototech patent, using chloroauric acid (16). The Pt/Li-NiO catalyst gave much better performance than Au/Li-NiO.

2.2 Transition Metal Oxides as Support Materials for O_2 Reduction Electrocatalysts

Transition metal oxides are of interest as alternative supports to carbon. Some of these oxides are quite stable in alkaline solution and have reasonable electronic conductivity. The effect of adsorbed CoTsPc on lithiated NiO for O_2 reduction was investigated using the rotating disk electrode (RDE) technique and gas-fed electrodes. In the RDE experiments, mosaic single-crystal NiO and polycrystalline NiO grown on a metallic Ni disk were used. A significant enhancement of the O_2 reduction kinetic current (~15 fold) on CoTsPc was observed in 0.1 M KOH at -0.4 V vs. Hg/HgO, OH^- at room temperature. The presence of CoTsPc in solution phase was necessary to obtain this effect. It was found that CoTsPc (negatively charged) was weakly bound to the electrode surface when it was adsorbed from an air-saturated aqueous solution (~5 x 10^{-5} M) with the electrode at open circuit and at low rotation rate (~100 rpm). A positively charged macrocycle, cobalt tetra kis-(4-trimethyl ammonium phenyl)

porphyrin also showed weak adsorption under similar conditions. This indicates that the excess negative charge (17, 18) on the NiO surface has practically no effect on the adsorption of the macrocycle.

Another reason for the weak adsorption may be because the NiO surface is covered by strongly bonded OH^- groups which prevent Ni^{+2} from binding other ligands. Efforts were made to bind to the OH^- group through hydrogen bonding using small organic molecules with various functional groups. Efforts were also made to interpret the effect of adsorption in terms of electrophoretic properties of the oxide including the isoelectric point.

The isoelectric point for lithiated NiO was determined to be at pH 9.7., and reported in the literature to be at pH 10.4 for undoped NiO (17). At pH>9.7 the surface of the Li-NiO is negatively charged and this would inhibit the adsorption of the negatively charged $(CoTsPc)^{-4}$ as experimentally found. On the other hand, adsorption was also weak at pH 1.4. Further, a macrocycle with peripheral tetra-alkylammonium groups also adsorbed only weakly on Li-NiO in alkaline solution. Thus it appears likely that adsorption is weak due to the difficulty of displacing strongly bound surface OH, OH^- or H_2O. Other approaches to assist in the adsorption process are being considered, including the use of ion-conducting polymer layers.

O_2-reduction on CoTsPc preadsorbed on $LaCoO_3$ powder obtained from Basic Volume Ltd., England, in alkaline solution was also investigated. The typical surface area and particle size of this perovskite are 10-30 m^2/g and 0.1-0.05 μm, respectively. Thin-porous-coatings (TPC) on the electrode was used to assess the activity. Cyclic voltammetry of the CoTsPc on $LaCoO_3$ showed a small rounded peak corresponding to the redox process Co(II)/Co(I), indicating

adsorption of CoTsPc on the $LaCoO_3$ substrate. The half-wave potential for O_2 reduction was ~100 mV more positive for CoTsPc adsorbed on $LaCoO_3$ than for substrate alone (Fig. 14). The limiting current approached the same value at more negative potential (-0.9 V vs. SCE) with and without CoTsPc on $LaCoO_3$, showing that the same number of electrons are involved in the reduction process. The positive shift of the potential for O_2 reduction with CoTsPc on $LaCoO_3$ may be due to further decomposition of the peroxide by CoTsPc inside the pores because of the slow diffusion of peroxide ions. The O_2 reduction currents with the perovskites as substrate are about twenty times less than that with high-area carbon as the substrate. This difference is attributed to the low surface area and low electronic conductivity with perovskite substrate. Similar results were obtained for O_2 reduction on CoTsPc adsorbed on $La_{0.5}Sr_{0.5}MnO_3$.

Efforts were also made to prepare high area, conductive metal oxides based on nickel. Such materials should be more stable than carbon as supports for O_2 reduction or for bifunctional electrocatalysts, especially at more positive potentials during O_2 generation.

Among the various methods used to prepare the high-area transition metal oxides, a new method was recently developed at Battelle Northwest Laboratories (19). This method, which has been referred to as the glycine-nitrate method, involves a rapid combustion-like reaction between glycine and transition metal nitrates, reaching 1000-1400°C for just a few seconds. This method was used to prepare the perovskite $LaNiO_3$, which is a metallic conductor. The conventional procedure, which involves thermal decomposition of the nitrates, typically yields powders with BET surface areas less than 5 m^2/g. Using the glycine-nitrate method, which involves a quick combustion step (≤5 s) and 450°C heat treatment

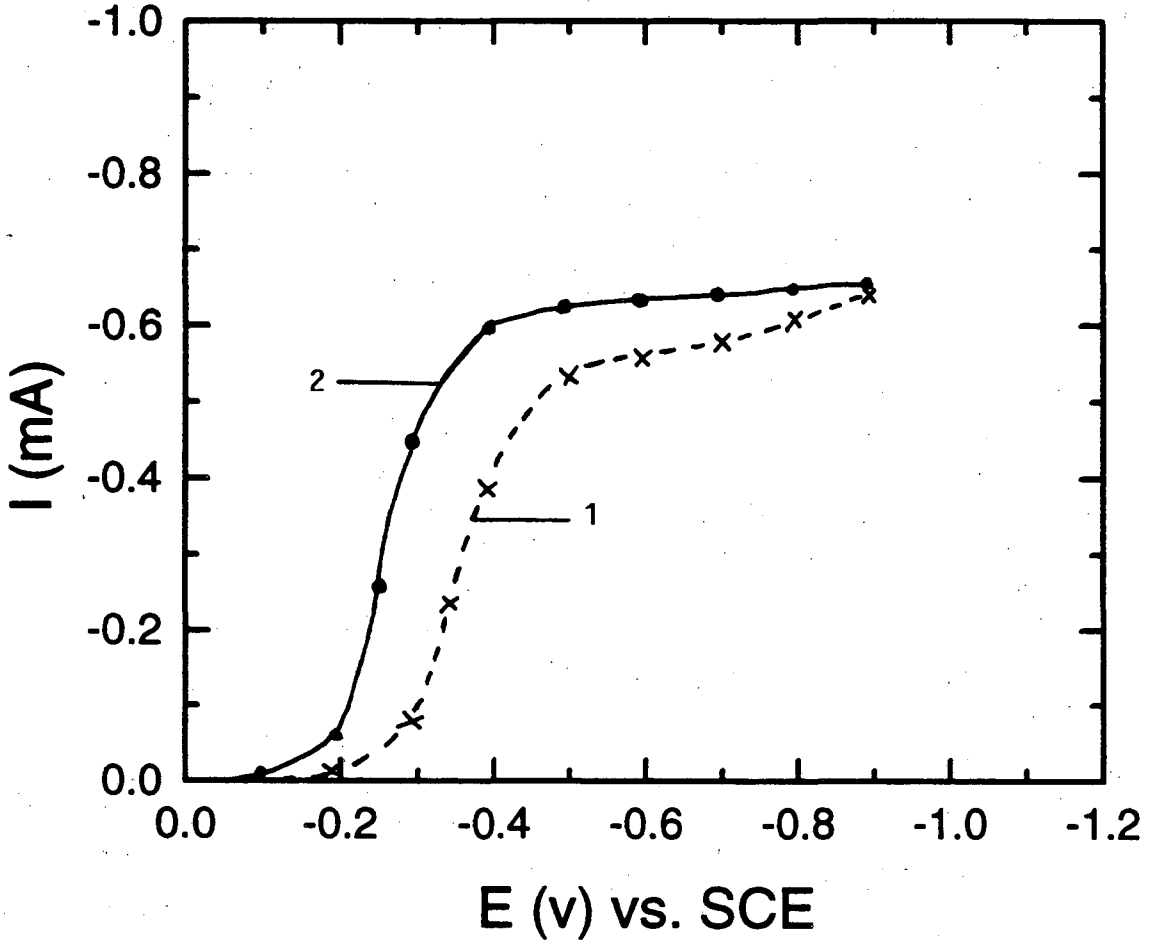

Fig. 14. Disk currents for O_2 reduction on a thin porous coating layer of $LaCoO_3$ (1) and CoTsPc adsorbed on $LaCoO_3$ (2) on OPG surface in O_2-saturated 0.1 M NaOH. Fluon (~10%) was used for the fabrication of the TPC electrode. Curves obtained point by point in the negative direction at room temperature.

Disk area (geometrical) = 0.45 cm^2
2500 rpm

in air, single-phase $LaNiO_3$ was obtained with a BET surface area of 15.3 m^2/g as shown by x-ray diffraction. This method appears to show promise for perovskite-type oxides in general, according to the developers (20).

Efforts were also continued to prepare higher area forms of lithiated nickel oxide, $Ni_{1-x}Li_xO$. The efforts were hampered by the need for higher heat treatment temperatures to enable the lithium to diffuse into the NiO particles. Undoped NiO can easily be prepared in high area form (≥100 m^2/g). A modified thermal decomposition in vaccum was used with $Ni(OH)_2$ and $CH_3CO_2Li.2H_2O$ as the starting materials followed by heat treatment in air at 350°C. The BET surface area was quite encouraging; ~23 m^2/g. The resistivity at room temperature and 34% theoretical denisty was ~20 Ωcm, which is also quite encouraging. (The resistivity decreases at higher tempéature). Since the X-ray diffraction pattern showed some evidence of particle size broadening effects, this material will be characterized shortly using EXAFS at Stanford in conjunction with Professor Daniel Scherson of CRWU.

The other support materials such as WC and SiC, in the powder form, were also used as substrates for cobalt tetramethoxy phenyl porphyrin (CoTMPP) as the catalyst. Porous gas-fed electrode measurements for O_2 reduction were made on these materials in 5.5 M KOH at 25°C with and without CoTMPP on the support and using NH_4HCO_3 as the pore former. The catalytic activity of CoTMPP for O_2 reduction was inferior to the activity of CoTMPP supported on a high-area carbon with or without heat treatment. This may be due to the larger particle size and lower surface area of these substrates as well as the poor conductivity as compared to the high-area carbons.

III. RESEARCH RECOMMENDATIONS

The following list summarizes research topics that should be considered:

1. Studies of factors controlling stability of precious metals and macrocycle catalysts including:
   - oxidation of carbon supports and ways of impeding oxidation by surface treatments such as selective fluorination and the use of certain carbons.
   - changes in the morphology and characteristics of the catalyst active layer.
   - sensitivties of oxygen catalysts to the transport of components of the anolyte into the catholyte.
   - use of ionomers to stabilize catalyst layers such as adsorbed macrocycles and UPD submonolayers
2. Studies of factors controlling activity of catalysts for oxygen reduction:
   - identification of intermediates, particularly adsorbed species
   - measurements of redox properties of reactants, intermediates and products both in solution-phase and as adsorbed species
3. Establish effective ways to bind transition metal to surfaces

IV. REFERENCES

1. B. Simic-Glavaski, S. Zecevic and E. Yeager, J. Am. Chem. Soc., 107, 5725 (1985).

2. W. C. Drinkard and J. C. Bailar, Jr., J. Am. Chem. Soc., 81, 4795 (1959).

3. B. N. Achar, G. M. Fohlen and J. A. Paker, J. Polym. Sci., 20 1785 (1985).

4. E. Yeager, "Oxygen Electrodes for Energy Conversion and Storage," Annual Report (1 October 1979 - 30 September 1980), Contract No. DEACO2-77-ET25502. Prepared by CWRU for Diamond Shamrock Corporation, November 1981.

5. E. Yeager, "Electrocatalysts for Oxygen Electrodes," Final Report, LBL No. 31278, prepared by CWRU for LBL, October 1991.

6. M.E. Peover and B. S. White, Electrochim Acta, 11, 1061 (1966).

7. D. T. Sawyer, G. Chiericato, Jr., C. T. Angelis, E. J. Nanni, Jr. and T. Tsuchiya, Anal. Chem., 54, 1720 (1982).

8. M. S. Hossain, Case Western Reserve University, Ph.D. Dissertation (1986).

9. E. L. Johnson, K. H.Pool and R. E. Hamm, Anal. Chem., 38, 61 (1968).

10. I. M. Kolhoff and T. B Reddy, J. Electrochem. Soc., 108, 980 (1961).

11. R. S. Nicholson, Anal. Chem., 37, 1351 (1965).

12. S. Gupta. C. Fierro and E. Yeager, J. Electroanal. Chem., 306, 239 (1991).

13. E. Yeager, "Electrocatalysts for O_2 Electrodes," Annual Report, LBL No. 26054, prepared by CWRU for LBL, August 1988.

14. H. G. Petrow and R. J. Allen, U.S. Patent 3,992,331, November 16, 1976.

15. H. G. Petrow and R. J. Allen, U.S. Patent 4,044,192, August 23, 1977.

16. H. G. Petrow, U.S. Patent 3,776,776, December 4, 1973.

17. G. A. Parks, Chem. Rev., 65, 177 (1965).

18. G. A. Parks and P. L. deBruyn, J. Phys. Chem., 66, 967 (1962).

19. L. A. Chick, L. R. Pederson, G. D. Maupin, J. L. Bates, L. E. Thomas and G. J. Exarhos, Mat. Let., 10, 6 (1990.

20. J. L. Bates, personal communication.

V. LIST OF RESEARCH PUBLICATIONS UNDER LBL/DOE PROJECT

1. "The Electrochemical Properties of Graphite and Carbon," E. Yeager, J. A. Molla and S. Gupta, Proceedings of the Workshop on The Electrochemistry of Carbon, Cleveland, Ohio, August 17-19, 1983, S. Sarangapani, J. R. Akridge and B. Schumm, eds., The Electrochemical Society, Pennington, NJ, 1984, pp. 123-157.

2. "Effect of Surface Treatment of Glassy Carbon on O_2 Reduction in Alkaline Solution," Z. W. Zhang, D. A. Tryk and E. Yeager, Proceedings of the Workshop on the Electrochemistry of Carbon, Cleveland, Ohio, August 17-19, 1983, S. Sarangapani, J. R. Akridge and B. Schumm, eds., The Electrochemical Society, Pennington, NJ, 1984, pp. 158-178.

3. "Carbon in Bifunctional Air Electrodes in Alkaline Solution," D. Tryk, W. Aldred and E. Yeager, Proceedings of the Workshop on the Electrochemistry of Carbon, Cleveland, Ohio, August 17-19, 1983, S. Sarangapani, J. R. Akridge and B. Schumm, eds., The Electrochemical Society, Pennington, NJ, 1984, pp. 192-220.

4. "Mechanisms for the Hydrogen and Oxygen Electrochemical Generation Reactions," Ernest Yeager and Donald Tryk, Hydrogen Energy Progress, Vol. V, T. N. Veziroglu and J. B. Taylor, eds., International Association for Hydrogen Energy, Pergamon Press, New York, 1984, pp. 827-844.

5. "In-situ Mossbauer Spectroscopy on an Operating Fuel Cell," D. Scherson, C. Fierro, E. Yeager, M. E. Kordesch, J. Eldridge, R. W. Hoffman and A. Barnes, J. Electroanal. Chem., 169, 287-302 (1984).

6. "Electrocatalysts for O_2 Reduction," E. Yeager, Electrochim. Acta, 29, 1527-1537 (1984).

7. "Mechanistic Aspects of Oxygen Electrochemistry," E. Yeager, D. Scherson, and B. Simic-Glavaski, Proceedings of the Symposium on The Chemistry and Physics of Electrocatalysis, San Francisco, California, May 8-13, 1983, J.D.E. McIntyre, M. J. Weaver, and E. Yeager, eds., The Electrochemical Society, Pennington, NJ, 1984, Vol. 84-12, pp. 247-270.

8. "In-situ Mossbauer Spectroscopy and Electrochemical Studies of the Thermal Stability of Iron Phthalocyanine Dispersed in High Surface Area Carbon," D. A. Scherson, C. A. Fierro, D. Tryk, S. L. Gupta and E. Yeager, J. Electroanal. Chem., 184, 419-426 (1985).

9. "Sauerstoffreduktionselektroden fur Elektrolyse - und Brennstoffzellen," R. Holze and E. Yeager, Technische Elektrolysen, Dechema Monograph, Vol. 98, No. 1993-2030, Verlag Chemie, Weinheim, 1985, pp 499-509.

10. "In-situ Spectroscopic Studies of Oxygen Electrocatalysts Involving Transition Metal Macrocycles," E. Yeager, D. Scherson, and C. Fierro, in Catalyst Characterization Science: Surface and Solid State Chemistry, M.L. Deviney and J.L. Gland, eds., ACS Symposium Series 288, American Chemical Society, Washington, DC, 1985, pp. 537-549.

11. "Spectroscopic and Electrochemical Studies of Transition-Metal Tetrasulfonated Phthalocyanines. 3. Raman Scattering from Electrochemically Adsorbed Tetrasulfonated Phthalocyanines on Silver Electrodes," B. Simic- Glavaski, S. Zecevic and E. Yeager, J. Am. Chem. Soc., 107, 5625-5635 (1985).

12. "Spectroscopic and Electrochemical Studies of Transition-Metal Tetrasulfonated Phthalocyanines." 6. The adsorption of Iron Tetrasulfonated Phthalocyanine on Single Crystal Silver Electrodes, R. Adzic, B. Simic-Glavaski and E. Yeager, J. Electroanal. Chem., 194, 155-163 (1985).

13. "Spectroscopic and Electrochemical Studies of Transition Metal Tetrasulfonated Phthalocyanines. 5. Voltammetric Studies of Adsorbed Tetrasulfonated Phthalocyanines (MTsPc) in Aqueous Solutions," S. Zecevic, B. Simic-Glavaski, E. Yeager, A.B.P. Lever and P.C. Minor, J. Electroanal. Chem., 196 (1985) 339-358.

14. "Catalytic Activity of Manganese Dioxide for Hydrogen Peroxide Decomposition in Alkaline Solutions," Y. Zalyoksnis, D. Tryk and E. Yeager, Proceedings of the 2nd International Battery Material Association, Vol. 2, Graz, 1985, pp. 467-476.

15. "Transition Metal Macrocycles Supported on High Area Carbon: Pyrolysis-Mass Spectrometry Studies," D. Scherson, A. A. Tanaka, S. L. Gupta, D. Tryk, C. Fierro, R. Holze, E. Yeager and R. P. Lattimer, Electrochim. Acta, 31, 1247-1258 (1986).

16. "Thermal Decomposition of Surfactants in PTFE-Dispersions," R. Holze, A. T. Riga and E. Yeager, J. Materials Science Letters, 5, 819-822 (1986).

17. "Dioxygen Electrocatalysis: Mechanisms in Relation to Catalyst Structure," Ernest Yeager, J. Molecular Catalysis, 38, 5-25 (1986).

18. "Heat-Treated Pyrrole Black-Based Electrocatalysts for O_2 Reduction," S. Gupta, D. Tryk, M. Daroux, W. Aldred and E. Yeager, in "Proceedings of the Symposium on Load Levelling and Energy Conservation in Industrial Processes," D. Chin, Editor, The Electrochemical Society, Pennington, NJ, 86-10, 207-218 (1986).

19. "Electrocatalytic Aspects of Iron Phthalocyanine and Its μ-Oxo Derivatives Dispersed on High Surface Area Carbon," A. A. Tanaka, C. Fierro, D. Scherson and E. B. Yeager, J. Phys. Chem., 91, 3799-3807 (1987).

20. "Spectroscopic and Electrochemical Studies of Transition-Metal Tetrasulfonated Phthalocya-nines. Part VIII. Spectroelectrochemical Studies of Stacked-Ring Silicon Phthalocyanines," B. Simic-Glavaski, A. A. Tanaka, M. E. Kenney and E. Yeager, J. Electroanal Chem., 229, 285-296 (1987).

21. "The Use of Electrochemical and Non-Electrochemical Methods for the Determination of Peroxide Decomposition Rate Constants," R. E. Carbonio, D. Tryk and E. Yeager, Proceedings of the Symposium on Electrode Materials and Processes for Energy Conversion and Storage, S. Srinivasan, S. Wagner and H. Wroblowa, eds., The Electrochemical Society, Pennington, NJ, Vol. 87-12, pp. 238-255 (1987).

22. "Electrochemistry of Iron Oxides: An in-situ Mossbauer Study," C. Fierro, R. E. Carbonio, D. Scherson and E. Yeager, J. Phys. Chem., 91 6579-6581, (1987).

23. "Perovskite-Type Oxides: Oxygen Electrocatalysis and Bulk Structure," R. E. Carbonio, C. Fierro, D. Tryk, D. Scherson and E. Yeager, J. Power Sources, 22, 387-398 (1988).

24. "In-situ Mossbauer Effect of a Spectroscopy Model Iron Perovskite Electrocatalyst," C. Fierro, R. E. Carbonio, D. Scherson and E. Yeager, Electrochim. Acta, 33, 941-945 (1988).

25. "Electrochemistry of Carbon Relative to Batteries and Fuel Cells," E. Yeager and D. Tryk, Proceedings of the 33rd International Power Sources Symposium, Cherry Hill, PA, June 13-16, 1988, The Electrochemical Society, Pennington, NJ, 1988, pp. 114-128.

26. "Heat-Treated Polyacrylonitrile-Based Catalysts For Oxygen Electroreduction," S. Gupta, D. Tryk, I. Bae, W. Aldred and E. Yeager, J. Applied Electrochem., 19 19-27 (1989).

27. "Oxygen Reduction on Adsorbed Iron Tetrapyridinoporphyrazine," A. A. Tanaka, C. Fierro, D. A. Scherson and E. Yeager, Materials Chemistry and Physics, 22, 431-456 (1989).

28. "Examination of the Ionomer/Electrode Interface using the Ferric/Ferrous Redox Couple," D. Chu, D. Tryk, D. Gervasio and E. Yeager, J. Electroanal. Chem., 272, 277-284 (1989).

29. "The Electrochemistry of Graphite and Modified Graphite Surfaces: The Reduction of O_2," M. S. Hossain, D. Tryk and E. Yeager, Electrochim. Acta, 34, 1733-1737 (1989).

30. "Electroreduction of Oxygen on Pyrolytic Graphite Electrode with Adsorbed Layer of Cobalt Tetrasulfonated Phthalocyanine in Acetronitrile and Dimethylformamide," H. Huang, D. Tryk and E. Yeager, Chem. J. Chinese Univ. 5, 164-170 (1989).

31. "Infrared Reflectance Absorption Spectroscopy (IRRAS). Study of the Thermal Stability of Perfluorinated Sulphonic Acid Ionomers on Pt," D. Chu, D. Gervasio, M. Razaq and E. Yeager, J. Appl. Electrochem. 20, 157-162 (1990).

32. "Infrared Spectroscopic Determination of pH Changes in Diffusionally Decoupled Thin-Layer Electrochemical Cells," I. T. Bae, D. Scherson and E. Yeager, J. Anal. Chem., 62, 45-49 (1990).

33. "Electrocatalysts for Oxygen Electrode in Fuel Cells and Water Electrolyzers for Space Applications," J. Prakash, D. Tryk and E. Yeager, J. Power Sources, 29, 413-422 (1990).

34. "ESCA and Electrochemical Studies of Chelate-Modified Carbon Materials for Cathode Oxygen Reduction," D. Ohms, S. Gupta, D. A. Tryk, E. Yeager and K. Wiesener, Z. Physik. Chem., 272, 451-459 (1990).

35. "The Effects of Cyanide on the Electrochemical Properties of Transition Metal Macrocycles for Oxygen Reduction in Alkaline Solutions," S. Gupta, C. Fierro and E. Yeager, J. Electroanal. Chem., 306, 239-250 (1991).

36. "In-Situ Infrared Spectroscopic Studies of Redox Active Self-Assembled Monolayers on Gold Electrode Surfaces," I. T. Bae, H. Huang, E. Yeager and D. A. Scherson, Langmuir, 7, 1558-1562 (1991).

37. "Oxygen Reduction on Poly(4-vinylpyridine)-Modified Ordinary Pyrolytic Graphite Electrodes with Adsorbed Coablt Tetra-sulphonated Phthalocyanine in Acid Solutions," Z. Y. Zeng, S. L. Gupta, H. Huang and E. Yeager, J. Appl. Electrochem., 21, 973-981 (1991).

38. "Studies of the Adsorption of Tetrasulfonated Phthalocyanines on Graphite Substrate," S. Gupta, H. Huang and E. Yeager, Electrochim. Acta, 36, 2165-2169 (1991).

VI. Ph.D. DISSERTATIONS UNDER LBL/DOE PROJECT

1. C. Fierro, "Transition Metal Macrocycles as Catalysts for the Electrochemical Reduction of O_2," Case Western Reserve University, May, 1985.

2. S. Hossain, "Oxygen Reduction on Carbon and Modified Carbon Surfaces," Case Western Reserve University, May, 1986.

3. A. Tanaka, "Electrochemical Properties of Transition Metal Macrocycles for Oxygen Reduction," Case Western Reserve University, May, 1987

4. D. Chu, "Studies of the Solid Polymer Electrolyte-Electrode Interface," Case Western Reserve University, May, 1989.

5. I. Bae, "*In-situ* Infrared Spectroscopic Studies of Electrocatalytic Systems," Case Western Reserve University, August, 1989.

6. J. Prakash, "Oxygen Electrocatalysis on Ruthenium Metal and its Pyrochlores," Case Western Reserve University, June, 1990.

7. H. Huang, "The Role of Adsorbed Species in Various Electrocatalytic Processes: Electrochemical and *In-situ* Infrared Spectroscopic Studies," Case Western Reserve University, May, January 1992.

Appendix A

This gives the list of various active catalyst systems prepared and examined for O_2 reduction and generation in alkaline and acid electrolytes with porous O_2-fed (1 atm) electrodes.

TABLE A-I

O_2 Reduction Polarization for Various Catalyst Systems in 4M NaOH at 60°C with Porous O_2-Fed (1 atm) Electrodes

Potential in mV vs Hg/HgO, OH^-

S. No.	Catalyst Systems	Red. Pot. (mV) at -100 mA cm^{-2}
	Transition Metal Macrocycles	
1.	10% CoTMPP/DRB (450°C HT)	-47
2.	10% CoTPP/DRB (450°C HT)	-81
3.	20% FeTMPP/DRB (800°C HT)	-38
4.	15%CoTAA/P-33 (650°C HT)	-51
5.	5% CoTMPP/SASB (450°C HT)	-70
6.	8.9% CoTMPP/SASB (800°C HT)	-65
7.	4.8% CoTMPP/XC-72 (450°C HT)	-70
8.	20% CoTMPP/BP (800°C HT)	-75
	H_2 TMPP + Metal Oxides	
9.	3% H_2TMPP/SB (450°C HT) + 10% Ru and Co as hydroxides	-42
10.	4.4% H_2TMPP/XC-72 + 2.5% Fe and Co as hydroxides (450°C HT)	-85
	Naturally Occurring Macrocycles	
11.	10% Hemine/DRB (800°C HT)	-73
12.	10% Chlorophyll/DRB + 2.5% Co as hydroxide (450°C HT)	-92
13.	40% PAN /XC-72 +10% $Co(OAc)_2$ (800°C HT)	-75

TABLE A-I
(continued)

O_2 Reduction Polarization for Various Catalyst Systems in 4M NaOH at 60°C with Porous O_2-Fed (1 atm) Electrodes

Potential in mV vs Hg/HgO, OH^-

S. No.	Catalyst Systems	Red. Pot. (mV) at -100 mA cm^{-2}
	Macrocycles + Perovskites	
14.	PB+2.5% $Co(OAc)_2$ (700°C HT)	-90
15.	PB + 2.5% Fe as acetate (850°C HT)	-88
16.	3% CoTMPP/SB (450°C HT) + $La_{0.5}Sr_{0.5}Co_{0.9}Ru_{0.1}O_3$	-58
17.	3% CoTMPP/SB (450°C HT) + $La_{0.5}Sr_{0.5}CoO_3$	-67
18.	3% CoTMPP/SB (450°C HT) + La-Fe Perovskite	-68
19.	5% CoOEP/XC-72 (400°C HT) + $La_{0.8}Sr_{0.2}Co_{0.9}Ru_{0.1}O_3$	-45
20.	15% CoTAA/P-33 (650°C HT) + $La_{0.5}Sr_{0.5}Co_{0.8}Ru_{0.2}O_3$	-48
21.	3% H_2 TMPP/SB (450°C HT) + $La_{0.8}Sr_{0.2}Co_{0.9}Ru_{0.1}O_3$	-56

TABLE A-I
(continued)

O_2 Reduction Polarization for Various Catalyst Systems in 4M NaOH at 60°C with Porous O_2-Fed (1 atm) Electrodes

Potential in mV vs Hg/HgO, OH^-

S. No.	Catalyst Systems	Red. Pot. (mV) at -100 mA cm^{-2}
	Polymers + Perovskites	
22.	40% PAN/XC-72 + 5% $Co(OAc)_2$ (800°C HT) + $La_{0.8}Sr_{0.2}Co_{0.9}Ru_{0.1}O_3$	-64
23.	40% PAN/SASB + 5% $Co(OAc)_2$(800°C HT) + $LaFe_{0.1}Ni_{0.9}O_3$	-72
24.	40% PAN/SASB + 5% $Co(OAc)_2$ (800°C HT) + $LaFe_{0.33}Co_{0.33}Ni_{0.33}O_3$	-68
	Platinum	
25.	10% Pt/XC-72 (Prototech electrode)	-53
26.	5% Pt/DRB (Electromedia electrode)	-51

DRB = De-ashed RB carbon (Calgon)
SB = Shawinigan black (Gulf)
SASB = Steam activated SB (Electromedia)
P-33 (East Germany)
XC-72 (Calgon)
BP = Black Pearls (Cabot)
CoTMPP = Cobalt tetramethoxy phenyl porphyrin
H_2TMPP = Metal-free tetramethoxyphenyl porphyrin
LBL = Lawrence Berkeley Laboratory carbon
TAA = tetraazaannulene
TPP = tetraphenyl porphyrin
PAN = Polyacrylonitrile
PAA = Polyacrylamide
PB = Pyrrole black
RAI = Anion exchange membrane
Co-OEP = Cobalt octaethyl porphyrin
DMDAAC = Dimethyldiallyl ammonium chloride

TABLE A-II

O_2 Reduction and Generation Polarization Data for Various Catalysts in 5.5M KOH at 22°C with Porous O_2-Fed (1 atm) Electrodes

Potentials in mV vs. Hg/HgO, OH^-

S. No.	Catalyst Systems*	Red. Pot. (mV) at -100 mA cm^{-2}	Oxi. Pot. (mV) at +10 mA cm^{-2}
1.	$Pb_2Ru_2O_{6.5}$/SB (air oxidized)	-75	474
2.	$Pb_2(Ru_{1.67}Pb_{0.33})O_{6.5}$/SB (air oxidized)	-16	477
3.	$Pb_2(Ru_{1.67}Pb_{0.33})O_{6.5}$/SB (air oxidized)/RAI membrane on E.S.	-23	442
4.	$Pb_2(Ru_{1.67}Pb_{0.33})O_{6.5}$/CoTMPP/SB	-32	447
5.	$Pb_2(Ru_{1.67}Pb_{0.33})O_{6..5}$/CoTMPP/SB/RAI membrane on E.S.	-38	449
6.	$Pb_2(Ru_{1.6}Pb_{0.33})$/SB (air oxidized)/ DMDAAC/Nafion	-15	462
7.	$Pb_2Ru_2O_{6.5}$(Self supported)	+10	459
8.	$Pb_2Ru_{1.5}Ir_{0.5}O_{7-y}$/SB (air oxidized)	-31	483
9.	$Pb_{1.5}Co_{0.5}Ru_2O_{6.5}$/SB (air oxidized)	-60	472
10.	3% CoTMPP/SB (450°C HT)	-67	—
11.	3% CoTMPP/SB (450°C HT) + $Pb_2Ru_2O_{6.5}$	-35	—
12.	3% H_2TMPP/SB (450°C HT) + 10% Co, Ru as hydroxides	-60	—
13.	3% H_2TMPP/SB (450°C HT) + 10% Co, 6.5% Fe + Ni as hydroxides	-75	—

*For notations, see Table A-I.

TABLE A-II
(continued)

O_2 Reduction and Generation Polarization Data for Various Catalysts in 5.5M KOH at 22°C with Porous O_2-Fed (1 atm) Electrodes

Potentials in mV vs. Hg/HgO, OH^-

S. No.	Catalyst Systems*	Red. Pot. (mV) at -100 mA cm^{-2}	Oxi. Pot. (mV) at +10 mA cm^{-2}
14.	3% H_2TMPP/SB (450°C HT) + Fe, Ni, Co perovskites	-87	606
15.	3% H_2TMPP/SB (450°C HT) + perovskite $La_{0.8}Sr_{0.2}Co_{0.9}Ru_{0.1}O_3$	-65	—
16.	3% H_2TMPP/SB (450° C HT) + perovskites: $La_{0.5}Sr_{0.5}Co_{0.5}Mn_{0.5}O_3$ + $Ni_{0.5}Ru_{0.5}LaO_3$	-75	—
17.	3% CoTMPP/SB (450°C HT) + perovskite $La_{0.8}Sr_{0.2}Co_{0.9}Ru_{0.1}O_3$	-85	598
18.	40% PAN + 5% $Co(oAc)_2$ + XC-72 (800°C HT)	-75	—
19.	5% CoOEP/XC-72 (400°C HT)	-85	—
20.	5% CoOEP/SASB (No HT) + perovskite $LaFe_{0,15}Ni_{0.85}O_3$	-75	612
21.	$LaFe_{0.15}Ni_{0.85}O_3$/DRB (No HT)	-65	—
22.	20% PAA + 40% PAN + 5% $Co(oAc)_2$ + XC-72 (800°C HT)	-70	—
23.	3% CoTMPP/SB (450°C HT) + pyrochlore $Pb_{1.5}Co_{0.5}Ru_2O_{6.5}$	-58	495
24.	1.5% CoTMPP/SB (450°C HT)	-70	—
25.	1.5% CoTMPP/SB (450°C HT) + pyrochlore $Bi_{1.5}Co_{0.5}RuIrO_{7-y}$	-66	574

*for notations, see Table A-I.

TABLE A-II
(continued)

O_2 Reduction and Generation Polarization Data for Various Catalysts in 5.5M KOH at 22°C with Porous O_2-Fed (1 atm) Electrodes

Potentials in mV vs. Hg/HgO, OH^-

S. No.	Catalyst Systems*	Red. Pot. (mV) at -100 mA cm^{-2}	Oxi. Pot. (mV) at +10 mA cm^{-2}
26.	$Pb_2Ru_2O_{6.5}$/SB (air oxidized)/RAI membrane on the E.S.	-20	464
27.	$Pb_2Ru_2O_{6.5}$ + NH_4HCO_3 (self supported)	+20	—
28.	10% Pt (Prototech)/$Pb_2Ru_2O_{6.5}$ + NH_4HCO_3	-10	—
29.	10% Pt/LBLcarbon (Prototech method)	-65	—

*for notations, see Table A-I.

TABLE A-III

O_2 Reduction Polarization Data for Various Catalysts in 85% H_3PO_4 at 100°C with Porous O_2-Fed (1 atm) Electrodes

Potential in mV vs RHE

S. No.	Catalysts*	Red. Pot. (mV) at -100 mA cm^{-2}
1.	10% FeTMPP/DRB (800°C HT)	680
2.	15% CoTAA/P-33 (650°C HT)	580
3.	4.75% CoTMPP/SASB (450°C HT) + Fluon + Nafion	570
4.	5% FeTMPP/XC-72 (800°C HT) + Fluon + Nafion	470
5.	10% CoTMPP/DRB (800°C HT)	670
6.	9.3% CoTMPP/SASB (800°C HT) + Fluon + Nafion	600
7.	10% Hemin/DRB (800°C HT)	650
8.	10% Pt/Consel (Powercat 2000)	640
9.	10% Pt/XC-72 (Prototech)	770
10.	10% Pt/XC-72 + SASB (CWRU Fabrication)	710
11.	10% Pt/XC-72 (Prototech) (CWRU Fabrication)	770
12.	5% Pt/DRB (EMC) (CWRU Fabrication)	650
13.	0.5 mg Pt/cm^2 (commercial, Prototech)	730
14.	0.5 mg Pt/cm^2 (commercial, Prototech) impregnated with Nafion	700
15.	Powercat 2000 (CWRU Fabrication)	760
16.	0.5 mg Pt/cm^2 (commercial, Prototech) impregnated with DOW compound	730

*For notations, see Table A-I.

TABLE A-IV

O_2 Reduction Data for Catalysts in 2.5 M H_2SO_4 and Nafion Membrane at 60°C

Potential in mV vs RHE

S. No.	Catalysts	BET Surface Area (m^2g^{-1})	Red. Pot. (mV) at -100 mA cm^{-2}
	Macrocycles (w/o Nafion)[a]		
1.	15% CoTAA/P-33 (630°C HT)	~1000	680
2.	20% CoTAA/BP (630°C HT)	~1400	700
3.	10% CoTMPP/DRB (800°C HT)	~1200	600
	Pyrochlores with carbon[b]		
4.	$Pb_2Ru_2O_{6.5}$ + SB	11	475
5.	$Pb_2Ru_2O_{6.5}$ + SB	56	475
6.	$Pb_2Ru_2O_{6.5}$ + SB	50	448
7.	$Pb_2Ru_2O_{6.5}$+ SB	3.5	383
	Pt doped pyrochlores[b]		
8.	$Pb_2Ru_{1.8}Pt_{0.2}O_{6.5}$	68	405
9.	$Pb_2Ru_{1.9}Pt_{0.1}O_{6.5}$	48	278
10.	$Pb_2Ru_{1.9}Pt_{0.1}O_{6.5}$	3.1	204
	Pt on supports[b]		
11.	Prototech Pt	—	806
12.	10% Pt/$Pb_2Ru_2O_{6.5}$	11	754

[a]at 25°C
[b]Pyrochlore with different BET surface area

Appendix B

This gives a list of various catalysts prepared and examined for the decomposition of peroxide in alkaline electrolytes.

TABLE B-I
Peroxide Decomposition Rate Constants for Selected Catalysts
in Alkaline Solution[a]

material (no. of determinations)[d]	decomposition rate constant,[b] $cm^3\ s^{-1}\ g^{-1}$	BET surface area $m^2\ g^{-1}$	hetero-geneous rate constant,[c] $cm\ s^{-1} \times 10^{-5}$
Co-based oxides			
$LaCoO_3$ (2)[d]	1.4	2.7	5.4
Co_3O_4 (475°C) (1)	2.2	-	-
Co_3O_4 (80°C) (1)	10.9	-	-
Co-Fe-based oxide			
$LaCo_{0.5}Fe_{0.5}O_3$ (1)	0.54	2.9	1.8
Co-Ni-based oxide			
$LaCo_{0.5}Ni_{0.5}O_3$ (1)	2.4	3.0	8.0
Co-Ru-based oxide			
$La_{0.8}Sr_{0.2}Co_{0.9}Ru_{0.1}O_3$ (1)	1.2	1.7	7.1
Cr-based oxide			
$LaCrO_3$ (1)	0.28	-	-
Fe-Ni-based oxides			
$LaFe_{0.1}Ni_{0.9}O_3$ (1)	6.6	-	-
$LaFe_{0.25}Ni_{0.75}O_3$ (1)	3.8	1.4	26.8
Fe-Co-Ni-based oxide			
$LaFe_{0.33}Co_{0.33}Ni_{0.33}O_3$ (3)	1.37	2.4	5.7
Ni-based oxide			
$LaNiO_3$ (1)	0.06	-	-
Mn-based oxides			
$LaMnO_3$ (1)	0.7	1.3	5.4
$La_{0.5}Pb_{0.5}MnO_3$ (4)	11.2	17.8	6.3
$La_{0.5}Sr_{0.5}MnO_3$ (3)	8.2	10.5	7.8
Co-macrocycles			
4.7 wt.% CoTMPP/XC-72 (no HT)[e] (1)	10.1	113	0.89
4.7 wt.% CoTMPP/XC-72 (800°C HT) (1)	44	295	1.5
Fe-macrocycles			
4.8 wt.% $(FeTMPP)_2O$/XC-72 (no HT) (1)	0.12	131	0.009
4.8 wt.% (FeTMPP)2O/XC-72 (800°C HT) (1)	34	173	2.0

Notes

a. 0.1 M NaOH.

b. The gasometric method was used. The sample was dispersed using ultrasonic agitation in 45 cm^3 NaOH solution for 1 min. and then stirred with a magnetic stir bar for 5 min. Then 5 cm^3 of 2 M H_2O_2 solution was added to the suspension, and the volume of evolved O_2 was monitored as a function of time. The ln $c_{HO_2^-}$ was plotted as a function of time, and the initial slope was used to evalutate the rate constants.

c. The heterogeneous rate constants were calculated by dividing the rate constants which were normalized to the weight of catalyst per unit volume of solution by the catalyst surface area in cm^2. One advantage of the heterogeneous rate constant is that it can be used to calculate expected O_2 reduction currents in gas-diffusion electrodes (assuming that the current is limited by the peroxide decomposition rate).

d. The number of separate measurements.

e. HT = heat treatment temperature for macrocycles on high-area carbon.

LAWRENCE BERKELEY LABORATORY
UNIVERSITY OF CALIFORNIA
TECHNICAL INFORMATION DEPARTMENT
BERKELEY, CALIFORNIA 94720